Research Square

Preprints are preliminary reports that have not undergone peer review.
They should not be considered conclusive, used to inform clinical practice,
or referenced by the media as validated information.

Dual Cation Cross-Linked Alginate-Kaolin Hydrogel Beads: A Sustainable and Powerful Toolkit for Enhancing Wastewater Remediation

Meriem Fizir

meriem.fizir@univ-dbkm.dz

Khemis Miliana University

Khawla Boussibeur

Khemis Miliana University

Amina Richa

Khemis Miliana University

Sami Touil

Khemis Miliana University

Liu Wei

Zhejiang Pharmaceutical University

Houda Douba

University of Khemis Miliana

Dilmi Asma

University of Khemis Miliana

Souad Cherifi

Khemis Miliana University

Houria Rezala

University of Khemis Miliana

Meryem Briki

University of M'Hamed Bougara Boumerdes

Jiawei Shi

Zhejiang Pharmaceutical University

Research Article

Keywords: Alginate, Kaolin, Chlortetracycline hydrochloride, Adsorption, Pharmaceutical wastewater, Surface wastewater

Posted Date: May 11th, 2026

DOI: https://doi.org/10.21203/rs.3.rs-9416526/v1

License: This work is licensed under a Creative Commons Attribution 4.0 International License.
Read Full License

Additional Declarations: No competing interests reported.

Dual Cation Cross-Linked Alginate-Kaolin Hydrogel Beads: A Sustainable and Powerful Toolkit for Enhancing Wastewater Remediation

Meriem Fizir [a,b*], Khawla Boussibeur [a,b], Amina Richa [a], Sami Touil [a], Liu Wei [c*], Houda Douba [b,d], Dilmi Asma [b], Souad Cherifi [a,b], Houria Rezala [b], Meryem Briki[e-f], Jiawei Shi[g*].

[a]*Laboratory of Precision Agriculture, Environment and Sustainable Development, Khemis Miliana University, Algeria.*

[b]*Laboratoire de Valorisation des Substances Naturelles, University of Khemis Miliana, Algeria*

[c]*Zhejiang Pharmaceutical University, Ningbo 315500, Zhejiang, China.*

[d]*Laboratory Physical Chemistry of Materials Interfaces Applied to the Environment, University of Saad Dahlab Blida 1, Algeria*

e Petrochemical Synthesis Laboratory, Faculty of Hydrocarbons and Chemistry.University of M'Hamed Bougara Boumerdes, Algeria
f Hydrocarbon Technologies Laboratory, Faculty of Hydrocarbons and Chemistry.University of M'Hamed Bougara Boumerdes, Algeria
g College of Food Science and Technology, Zhejiang Pharmaceutical University, Ningbo 315500, Zhejiang, China

Email of the corresponding authors: liuwei_fj1992@163.com/meriem.fizir@univ-dbkm.dz/shijw@sina.cn

ABSTRACT

The research focuses on the removal of chlortetracycline hydrochloride (CTC) from water using a sustainable functional material designed as a toolkit, consisting of dual cation cross-linked alginate beads that incorporate kaolin (Fe/Ca-Alg@K). Key findings include: (1) the beads incorporate 3 g of K (Fe/Ca-Alg@K3), effectively adsorbed CTC; (2) an optimal dosage of 200 mg of beads achieved a notable removal rate of 95.12% at an initial concentration of 50 mg/L; (3) the pH level of the solution slightly affected the adsorption process; (4) the kinetic data aligned well with both pseudo-first-order and pseudo-second-order models, with physisorption being the dominant mechanism; (5) isotherm studies indicated that the adsorbent followed the Langmuir model, achieving a highcorrelation(R^2 = 0.94) and a maximum uptake of 156.46 mg/g at 318 K; (6) the inclusion of Kin the Alg matrix notably enhanced the adsorbent's reusability; (7) the presence of high concentration of various ions slightly reduce the removal of CTC; (8) XPS analysis revealed that the adsorption mechanism of CTC involved several interactions involving both the functional groups of beads and the silicon component of K; (9) these beads have the potential to reduce chemical oxygen demand (COD) to acceptable levels in pharmaceutical and surface wastewaters.

Keywords: Alginate; Kaolin; Chlortetracycline hydrochloride; Adsorption, Pharmaceutical wastewater, Surface wastewater.

1. Introduction

The widespread presence of residual antibiotics in the environment systems has become a critical global issue, garnering significant scientific and public attention [1]. Tetracycline antibiotics are recognized for their extensive effectiveness against a variety of bacteria, including both Gram-positive and Gram-negative types, spirochetes, obligate intracellular bacteria, and protozoan parasites. The earliest tetracyclines were naturally occurring substances obtained from the fermentation processes of actinomycetes. Chlortetracycline, which is produced by Streptomyces aureofaciens, was initially identified by Benjamin Duggar at Lederle Laboratories in 1948 and received approval for clinical use in the same year [2]. The hydrochloride form (CTC) was subsequently developed for clinical use. Due to bactericidal properties, tetracyclines including CTC are widely used in veterinary medicine to enhance livestock growth and prevent infectious diseases.However, because of their poor absorption and metabolism in vivo, tetracyclines can be transmitted directly into the environment through feces and urine as active ingredients [3]. The primary impacts of tetracyclines on the environment and living organisms can be summarized as detrimental effects on ecosystem functions and productivity. Additionally, they contribute to the emergence of antibiotic resistance genes and facilitate the transmission of these resistance genes through the food chain [4]. Before discharging wastewater into the environment, antibiotic residues need to be removed but it usually involves high cost. While processes like advanced oxidation can transform antibiotic molecules into simpler compounds or even fully mineralize them, these methods are expensive and challenging to implement for the comprehensive removal of antibiotics at an industrial level [5]. Consequently, physicochemical technologies are emerging as effective treatment solutions for organic contaminants [6]. Adsorption processes are commonly employed to extract organic pollutants from contaminated streams by adhering them to adsorbent surfaces [7]. However, their application in antibiotic removal has been documented for only about 30 compounds. The effectiveness of adsorption is significantly influenced by the type of adsorbent, the properties of the adsorbate, and the composition of the waste stream[8]. Various adsorptive materials, including activated carbon (AC)[9], carbon nanotubes (CNTs)[10], natural clays like bentonite[11], as well as MgO nanoparticles and ZnO-MgO nano-composites[12], are among the most frequently used options.

Kaolin has garnered significant attention as natural clay with abundant resources, low cost, and widespread availability in rocks worldwide[13-15].Kaolin is a clay mineral, with the chemical formula$Al_2Si_2O_5(OH)_4$. *It* is classified asa hydrous aluminum phyllosilicate [16]. Typically,its crystalline structure characteristically displays platy morphology, where oxygen atoms from one crystal layer facing the basal plane composed of hydroxyl groups in the adjacent layer[17].In addition to being biocompatible and cost-effective, kaolin features high porosity, distinctive compositions rich in hydroxyl groups on its surface, and a large specific surface area. These properties enable kaolin to effectively interact with a wide range of organic and inorganic molecules[18, 19].Kaolin has demonstrated a high removal rate for CTC[20, 21]. However, despite these encouraging findings, it has some limitations, such as the pressure drop generated by fluid filtration and the difficulty in recovering the material, which limits its practical use.Recently, researchers focus on using biopolymer composite beads to address these limitations. Among them sodium alginate (SA), which is an anionic polysaccharide mainly obtained from brown algae belonging to the Phaeophyceae family. It consists of (1,4) linked β-D-Mannuronate and α-L-Guluronate units. The ratio of Mannuronate to Guluronate (M/G) and the sequence of these units can differ depending on the extraction method, resulting in the presence of both homogeneous (GG or MM) and heterogeneous segments (GM or MG) within the same polymer chain. At a pH of 3.5, the carboxylate groups undergo protonation, which enhances strong interchain interactions through hydrogen bonding. Additionally, the carboxylate groups can interact significantly with cationic species at the supramolecular level, leading to the formation of complexes with a variety of geometrical structures.This chain reassembling, referred to as crosslinking, involves monovalent, divalent, trivalent, and tetravalent cations, providing a simple approach for creating hydrogels[22]. Alginate (Alg) with biocompatibility, hydrophilicity, and biodegradability was usually applied for adsorbent [23].However, the weak reusability performances of Alg beads have implications for its practical application. Our research group has been proven that incorporating clay minerals into biopolymers can substantially boost the mechanical stability and reusability of materials. Kaolin has the layered structure, which is more conducive to reinforce Alg matrix and make it have stronger durability and stability in the process of regeneration, suitable for practical applications[24].

Clay minerals like kaolin and montmorillonite (Mt) possess a layered structure that can strengthen the alginate matrix, enhancing its mechanical properties[25]. This reinforcement contributes to the durability and stability of the composite beads during the regeneration

process, making them more suitable for practical applications[26]. The selection of kaolin in this study is based on its stability, cost-effectiveness, and availability. Kaolin maintains stability across various clay mineral environments and is less susceptible to swelling compared to montmorillonite.This stability is beneficial for adsorption processes that require the clay's maintained the structural integrity. In contrast, Mt exhibits greater susceptibility to swelling and structural modifications, potentially compromising its long-term adsorption performance and stability. Furthermore, kaolin often presents practical advantages over montmorillonite in terms of both material availability and cost efficiency,making it a more favorable choice as an adsorbent[27].

In this context, this study investigates the effect of Fe/Ca-Alg@K beads on CTC removal from aqueous solutions in batch experiments. The iron and calcium employed for cross-linking the alginate are designed to interact with kaolin's negatively charged surfaces rather than depending only on conventional Ca^{2+} for the cross-linking, Fe^{3+} is also utilized,as iron oxides and iron-based clays are recognized as efficient adsorbents for organic contaminants and other pollutants[28, 29]. By using dual cross linked Alg based K beads, the removal efficiency of CTC is expected to be boosted along with the swelling efficiency. The innovative use of Fe/Ca cross-linked Alg@K beads for effectively removing CTC from wastewater has yet to be explored in existing literature. CTC sorption tests were conducted under various experimental conditions, including the physical state of the beads, the dosage of K clay in the beads, type of cross linkers, adsorbent dosage, solution pH, shaking speed, contact time, initial CTC concentration, temperature, co-existing ions, and organic pollutants. Kinetic and isotherm models were applied to fit the experimental data to assess the performance of the adsorption process. The results demonstrated that the Fe/Ca-Alg@K beads have a significant potential for CTC removal.

Materials and Methods

1.1. Chemicals and reagents

Sodium hydroxide (NaOH), sodium alginate (SA,$NaC_6H_7O_6$), iron (III) chloride ($FeCl_3$), hydrochloric acid (HCl), calcium chloride ($CaCl_2$), potassium chloride (KCl),sodium chloride (NaCl), sodium sulfate (Na_2SO_4), potassium nitrate (KNO_3), paracetamol, phenoxymethylpenicillin, diclofenac sodium was purchased from Sigma-Aldrich. Chlortetracycline hydrochloride (CTC)with the chemical formula "$C_{22}H_{24}Cl_2N_2O_8$" and a molecular mass of 515.34g/mol was acquired from Merck Chemicals (Darmstadt, Germany).

Kaolin clay (BiochemChemopharma, France) was used as received. The Direct-Q 3UV purification system was utilized for water generation, and all chemicals used were of analytical grade. The energy dispersive spectroscopy (EDS) of K (**Fig. S1**) showed the characteristic peaks of the different elements in this clay. The main elements observed are a predominant peak of silicon (Si), indicating high silica content, a significant peak of aluminum (Al) corresponding to its presence in the octahedral layer, and an intense oxygen (O) peak, reflecting its abundance in the silica tetrahedra and alumina octahedra. Weak peaks of trace elements such as calcium (Ca), sulfur (S), magnesium (Mg),sodium (Na), potassium (K), and carbon (C) were also observed, suggesting the presence of impurities [30].

1.2. Preparation of Alg@K beads

The beads with different composition were designed using the extrusion approach in the presence of Fe^{3+}/Ca^{2+} ions[15]. Taking Fe/Ca-Alg@K-3 as an example, the alginate beads were synthesized as follows: 2 g of SA was dissolved in 100 mL of double-distilled water, and the mixture was stirred for 1 h at 298 K to create agel. Next, 3 g of K was added to the gel and stirred continuously until a homogeneous Alg-K solution was achieved.Using a syringe,the solution containing SA and K was then slowlydripped intoa mixed iron(III)/calcium chloride solution (2% w/v).The mixed $FeCl_3/CaCl_2$solution (2%)was prepared as follows: 5 g of calcium chloride and 5 g of iron chloride were dissolved separately in 250 mL of double-distilled water. The two prepared solutions were then mixed in a 500 mL beaker. Fe/Ca cross-linked Alg@K was generated immediately when the alginate-kaolinsuspension interacted with the Fe^{3+}/Ca^{2+} solution. After solidification, the beads were thoroughly cleaned using distilled water to eliminate any excess $FeCl_3$ and $CaCl_2$ until the pH reached 7. Some of the resulting beads were stored in distilled water,while others were dried at 333K.For the preparation of alginate beads, the process was carried out similarly, but without the addition of kaolin. Mass composition of $FeCl_3$ and $CaCl_2$ for all designated samplesare summarized in **Table.1**. Preparation method of beads is depicted in **Fig. S2**.**Fig. 1** illustrates the potential cross-linking mechanism of Fe^{3+}/Ca^{2+} with the Alg matrix, as well as their binding behavior with the surface of K. Fe^{3+} binds to both GG (guluronate) and GM (mannuronate) groups, while Ca^{2+} specifically binds to GG groups, forming the characteristic egg-box structure[22]. Additionally, Algmay interacts with K minerals through hydrogen bonding and electrostatic interactions, enhancing the overall

stability and functionality of the composite material.Photograph image of the prepared beads with different K doses is presented in **Fig.S3**.

Table 1 Mass composition of $FeCl_3$ and $CaCl_2$ for all designated samples.

Sample designation	**Concentration of alginate (%)**	**Concentration of kaolin (%)**	**$FeCl_3$/$CaCl_2$ (wt./wt.)**
Fe/Ca-Alg	2	/	5/5*
Fe-Alg@K	2	2	10/-
Ca-Alg@K	2	2	-/10
Fe/Ca-Alg@K	2	2	5/5
Fe/Ca-Alg@K-3	2	3	5/5
Fe/Ca-Alg@K-4	2	4	5/5

* The mixture included 5 g of iron chlorideand 5 g of calcium chloride.

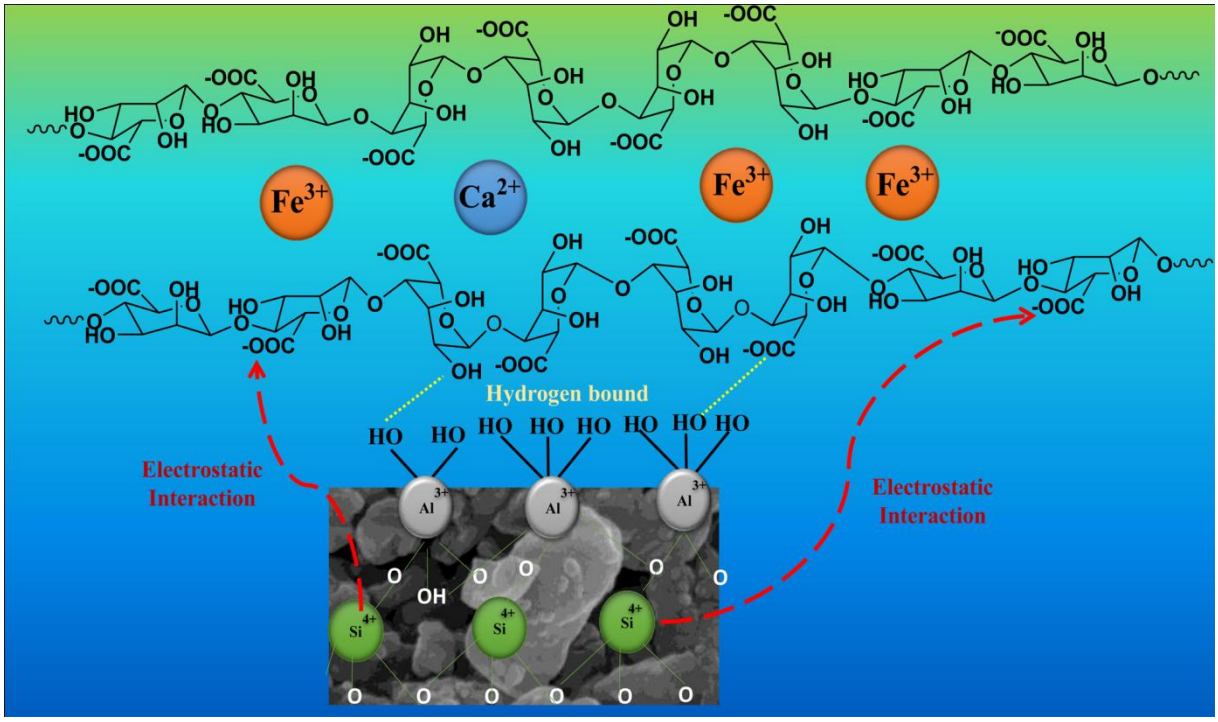


Fig.1 Cross-linking of Fe^{3+} and Ca^{2+} to the alginate framework and interaction with the surface clay mineral.

1.3. Determination of pH_{PZC} of Fe/Ca-Alg@K

The point of zero charge values of the investigated adsorbent was assessedusing the salt addition process. Briefly, 0.5 g of beads wasaddedto 20 mL of 0.01 M NaCl after adjusting the pH of the solutions with a base or acid, and then agitated for 24 h at 298K and 160 rpm. After the centrifugation process, the final pH was determined in each flask.The pH final versus pH initial plot was traced to determine the pH_{PZC} value of Fe/Ca-Alg@K [31].

1.4. Characterization

X-ray diffraction patterns of K and beads reveal absorption peaks at 2θ =10 to 90° at 298Kby a Bruker D8 ADVANCE with Cu Kα radiation at a voltage of 40 kV and a current of 30 mA with maximum crystallite size at 24.86°. FTIR analyses of K and Fe/Ca-Alg@K were performed on anFT-IR-8400 spectrometer (SHIMADZU).SEM(THERMOSCIENTIFIC QUATTRO S) was used to examine the surface morphology of both prepared beads andkaolin clay.To analyse the elemental composition of the kaolin clays, EDSwas conducted with an Ultra Dry silicon drift detector coupled tothe NORAN System 7 X-ray microanalysis (NSS-212e,ThermoFisher Scientific, Madison, WI). The XPS data was acquired utilizing an electron spectrometer manufactured by Thermo (ESCALAB 250Xi, USA).

1.5. Adsorption studies

2.5.1. Parameterstudies of CTC removal

The CTC removal performance of beads was systematically examined using batch adsorption experiments.The influence of key operational parameters on CTC adsorption efficiency was systematically investigated,including the physical state of the beads (wet and dried), type of cross-linkers used (Fe, Ca, and Fe/Ca), dosage of K clay in the beads (2 to 4 g), contact time (10-240 min), adsorbent dosage (100-1000 mg, wet beads), pH (2-12), initial CTC concentration (10-200 mg/L), shaking speed (100-250 rpm), and temperature (298-328K),were systematically optimized. A specific quantity of beads was combined with 10 mL of CTC solutions in flasks, with initial concentrations and pH values held constant.pH adjustments were made using dilute acid/base solutions, followed by constant agitation (200 rpm) at controlled temperature for predetermined contact time.Once equilibrium was achieved, the samples were centrifuged, and the supernatant analysed for CTC concentrationusing a Spectroquant Prove 300 spectrophotometer (model D-64293) at λ_{max} = 365 nm[23]. The adsorption capacity (Q, mg/g) and removal rate (%) of the adsorbents were calculated using equations (1) and (2):

$$Q = \frac{(C_0 - C_e) \times V}{m} \quad (1)$$

$$R(\%) = \frac{(C_0 - C_e) \times 100}{C_0} \quad (2)$$

Where C_0 and C_e (mg/L) are the initial and equilibrium CTC concentrations in the solutions, respectively. V is the volume (mL) of the aqueous solution, and m is the mass (g) of the adsorbents.To assess the measurements' reproducibility.All experiments were carried out in triplicate, and the average values were reported.

For the kinetic study, 200 mg of beads were brought into contact with 10 mL of CTC solution at concentrations of 25 and 50 mg/L for each flask. They were placed on a shaker with a regulated speed of 200 rpm and a pH 4at 298 K for 3h.The pseudo-first-order (PFO) and pseudo-second-order (PSO) models were applied to describe the adsorption kinetics of CTC onto the beads and todetermine the adsorption diffusion model. The non-linear equations for each model arelisted in **Table S1**.

To evaluate the adsorption isotherms, 200 mg of beads were added to CTC solutions with concentrations from 10 to 200 mg/L, maintaining a pH of 4 and temperatures of 298, 308, 318, 323, and 328 K. The adsorption equilibrium of CTC on the beads was characterized using the Freundlich andLangmuir models. The non-linear equations for both models are included in **Table S2**. The thermodynamic parameters ΔG° (standard free energy), ΔH° (standard enthalpy change), and ΔS° (standard entropy change) were calculated to assess the energy changes associated with the sorbent material and the sorption mechanism following adsorption. These parameters can be determined using the equations outlined in the Van't Hoff equation [32].

$$\Delta G° = \Delta H° - T\Delta S° \quad (3)$$

$$\mathrm{Ln}\ K_c = \Delta S/R - \Delta H/RT \quad (4)$$

$$K_c = Q_e/C_e \quad (5)$$

With $K_c$isthe equilibrium constant, $C_e$is the initial concentration of the adsorbent, Q_e isthe adsorption capacity, T isthe temperature (K) and R is an ideal gas constant (8.314 J/mol K).

2.5.2. Effect ofco-existing organic compounds and ions

To examine the influence of various co-existing organic compounds and ions on the adsorption of CTC onto the composites, tests were performed using 200 mg of beads and 10 mL of binary/multi-element solutions at pH 4.For the co-existing organic compounds study, the solutions contained 50 mg/L of potential interfering organic pollutants. The binary solutions were prepared by mixing CTC with phenoxymethylpenicillin, paracetamol, or diclofenac sodium,while the multielement solutions included CTC, phenoxymethylpenicillin (Mix 1), CTC, paracetamol (Mix 2), CTC, diclofenac sodium (Mix 3), CTC, paracetamol, and phenoxymethylpenicillin (Mix 4), CTC, phenoxymethylpenicillin, and diclofenac sodium (Mix 5), CTC, paracetamol, and diclofenac sodium (Mix 6), and CTC, paracetamol, diclofenac sodium, and phenoxymethylpenicillin (Mix 7). While for the co-existing ions study, the solutions contained 0.1 mol/L of potential interferingions. The binary systems were formed by mixingCTC with Ca^{2+}, Cl^{-}, SO_4^{2-}, or NO_3^{-}. Whereasthe multi-componentmixtures containing all species(CTC, Ca^{2+}, Cl^{-}, SO_4^{2-}, and NO_3^{-}. The mixtureswere stirred using a shaker set at a speed of 200 rpm for 3 h, centrifuged for 5 min at a speed of 3000 rpm, and then the solution concentrations were measured by a UV-VIS spectrophotometer.

2.5.3. Regeneration study

For an effective adsorbent, stability and cost-efficiency are vital features. To verify these properties, a regenerationtest was performed. The Fe/Ca-Alg@K-3 and Fe/Ca-Alg beads, after adsorbing CTC,underwent six regeneration cycles to assess theirreusability. The regeneration test involved immersing the beads for 1 h in a mixed solution of 20 mL 0.1 M HCl, 20 mL 0.1 M NaCl, and 20 mL DW. Afterwards, they were removed from the solution, rinsed thoroughly with distilled water, and prepared for testing in the next cycle.

1.6. Application of the beads in the real wastewaters

To examine the performance of the beads in removing organic pollutants from actual wastewaters, chemical oxygen demand (COD) removal experiments were conducted. The pharmaceutical wastewaters were collected from the industrial group of *SAIDAL*in the city of Medea, Algeriaand the surface water from *OuedChlef*in the city of Chlef, Algeria. The properties of these actual wastewater samples are detailed in **Table S3**.As the COD of the surface wastewaters is near the permissible limits of discharge, the test is carried out only on the pharmaceutical wastewaters.Different dosages of beads (100, 200, and 500 mg) were added to the pharmaceutical wastewaters (without filtration) and agitated at 200 rpm for 3 h at 298 Kto evaluateCOD removal.COD removal process details are presented in **TextS1**.

1.7. Application of the beads in the real pharmaceutical and surface wastewaters spikedwith CTC

In this experiment, 10 mL of pharmaceutical and surface wastewater was enriched with initial CTC concentrations of 50 and 100 mg/L.Then, 100 and 500 mg of beads were added at a temperature of 298 K and pH 4. The mixture was agitated for 3 h. The residual concentration of CTC was determined using UV-VIS spectrometry.

2. RESULTS AND DISCUSSION

2.1. Characterization

FT-IR analysis was performed to describe the surface functional groups of Fe/Ca-Alg@K-3 adsorbent, andthe results are presented in **Fig.2(a-b)**.The sodium alginate spectrum exhibited characteristic bands at 3410.26 cm^{-1} (-O-H stretching vibration), along with asymmetric and symmetric carboxylate ($-COO^-$) vibrations at 1620.26 cm^{-1} and 1427.37 cm^{-1}, respectively [33]. For the FT-IR spectrum of K, the -OH elongation bands were obtained at 3626.29 and 3487.42 cm^{-1},ascribedto the -OH grafting on the Al site of the K clay. Si-O-Si asymmetric stretching [34] and Si-O bending vibrations in the K were observed at 1033.88 and 1635.69 cm^{-1}, respectively. Furthermore, the Al-OH deformation vibration in K clay was detected at 933.58 cm^{-1}, these results matched the FT-IR characteristic absorption peaks of kaolinite[35].

The vibration bands of SA and K were preserved in the FT-IR spectrum of the Fe/Ca-Alg@K-3,indicating the coherence between these two materials. The asymmetric stretching vibration of a carboxylate was shifted to higher wavenumbers in Fe/Ca-Alg@K-3 composite beads (1627.97 cm^{-1}) compared to sodium alginate (1620.26 cm^{-1}) due to the introduction of K clay mineral[15].The Ca-O and Fe-O vibration bands were identified at 540.09 and 462.93 cm^{-1}[36, 37] in the Fe/Ca-Alg@K-3 beads, which confirms the good cross-linking of alginate by iron and calcium. In FT-IR spectra of CTC adsorbed by Fe/Ca-Alg@K-3, most of the prominent FT-IR bands of composite were preserved, with shifts in wavenumbers confirming successful CTC adsorption[38]. The availability of -OH functional groups in alginate and kaolin are responsible for the adsorption of CTC, while the Si–OH groups on kaolin can also promote the adsorption by hydrogen bounds.

The XRD patterns for K and composite beads are shown in **Fig. 2c**, recorded from 2θ = 10 to 90°. The observed absorption peaks are located at 2θ = 12.36°, 20.43°, 21.42°, 24.86°, 35.90°, and 38.46° [39]. The largest crystallite size is indicated by the peak at 24.86°. The 2θ values for kaolinite (Kaol) minerals are 12.36° and 24.86°, aligning with findings from previous studies [40].Additionally, the 2θ diffraction angle for quartz appears at 26.6° [41]. The results indicate that the diffraction peaks for the beads are less intense than those for K, suggesting that kaolin is evenly distributed within the gel beads.

.

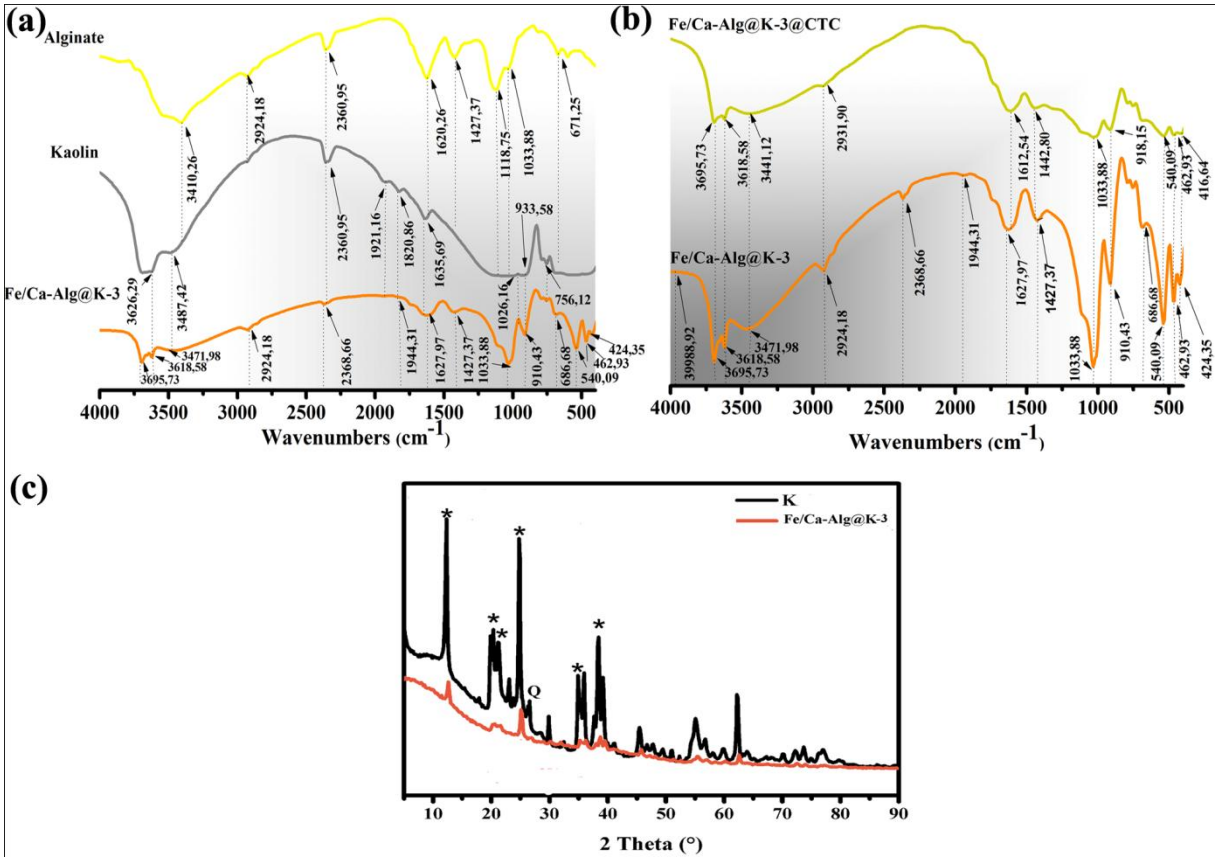


Fig.2 FT-IR spectra of (a)Fe/Ca-Alg@K-3 beads,kaolin, and sodium alginate; (b) Fe/Ca-Alg@K-3 before and after the adsorption of CTC; and (c) XRD patterns of Fe/Ca-Alg@K-3 beadsand K.

To examine the surface morphology of Fe/Ca-Alg@K-3, Alg beads, and Kduring the CTC sorption process, SEM analysis was performed. As shown in Fig. 3a, K features irregular crystalline structures with rough surface edges, measuringapproximately 0.2 μm in particlesize[42]. In contrast, the SEM images of the dry alginate beads (**Fig. 3b**) indicated that they had a spherical shape, measuring 1-1.5 mm in diameter, and displayed a smooth, opaque

surface. The SEM analysis of the Fe/Ca-Alg@K-3 composite beads, following the addition of K (**Fig. 3c-d**), revealed that the surface became irregular, exhibiting cracks, undulations, folds, and pores, resulting in an increased specific surface area.Consequently, both the accessible surface area and contact opportunity between CTC molecules and Fe/Ca-Alg@K-3 composite beads were increased. After CTC adsorption, the pleated voids becamefilled withnumerousfine particles**(Fig. 3e-f)**, which may becreated by the deposition of CTC on the adsorbent surface through local supersaturation[30],resulting in a non-uniform microstructure on the surface of the beads, characterized by polyhedral particles of different sizes.

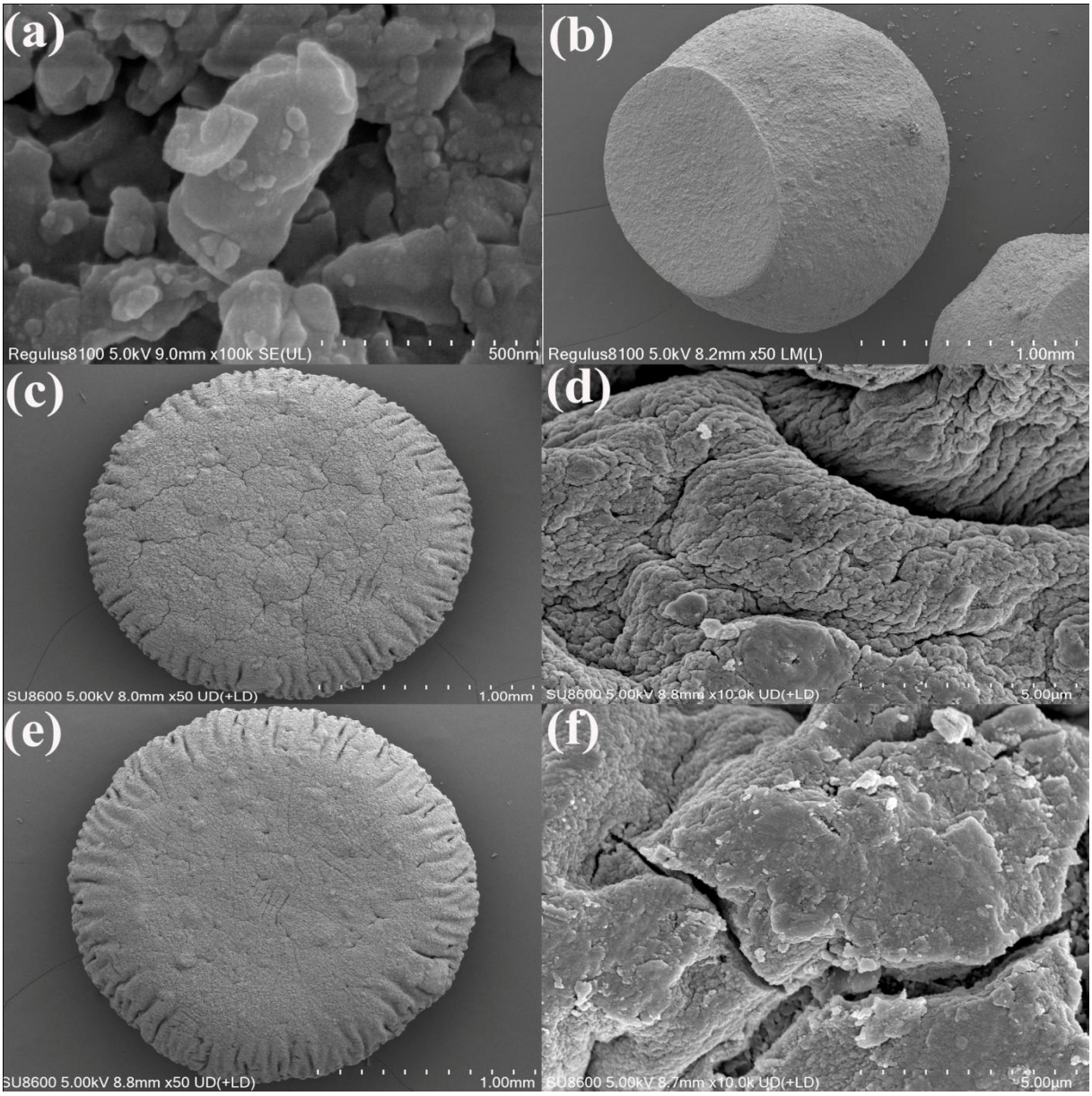


Fig.3 (a)SEM images of K; (b) Alg beads; (c-d) Fe/Ca-Alg@K-3; and (e-f) Fe/Ca-Alg@K-3@CTC.

2.2. Adsorption Study

3.2.1. The effect of the beads'physical state and the type of cross-linkers

The effect of the physical state of the synthesized beads on the adsorption of CTC was investigated**(Fig. 4a)**. The observed difference between the dried and humid states of the beads is attributed to the drying process. When the beads are dried, their porosity becomes insufficient for CTC to reach the active sites within the beads. Previous studies by Vincent Rocher et al., have reported that dried alginate beadswithactivated carbon andcontaining magnetic nanoparticles have low porosity based on measurements using the BET technique, indicating limited adsorption capacity. Drying the beads in an oven results in the closure of the porous volume and a significant reduction in pore size within the alginate matrix[43]. This irreversible transformation is primarily due to the rigidity imparted by calcium-ion cross-linking. Similar observations were made by Rassis et al., who found that drying calcium alginate gels containing bentonite led to significant densification and smaller pore sizes[44]. In contrast, the removal rate of CTC was higher when the beads were in the humid state, reaching a maximum of 91.875% in Fe/Ca-Alg@K beads. This improvement can be attributed to the presence of a large mass of water within the humid beads, which adds weight and contributes to the adsorption process[43]. Further investigation was conducted on the adsorption of CTC on Alg@K cross-linked with various metal cations, including Ca^{2+}, Fe^{3+}, and a mixture of Ca^{2+} and Fe^{3+}**(Fig. 4a)**. The results showed that the mixed Fe/Ca-Alg@K beads and Fe-Alg@K beadsdemonstrated a greateruptake of CTC compared to Ca-Alg@K beads. This may be attributed to the dual cross-linking potential of Fe and Ca and clearly demonstrates the advantage of the Fe^{3+}containing alginate hydrogels. Fe^{3+} can form complexes with CTC through coordination bonds. The OH and COOH groups present in CTC can act as ligands and coordinate with the Fe^{3+} ion, forming a complex. In addition, Fe^{3+} ions generally form stronger complexes with CTC compared to Ca^{2+} ions. This is due to the difference in the charge of the metal ions. Fe^{3+} is a trivalent cation, while Ca^{2+} is a divalent cation. The higher charge of Fe^{3+} allows for stronger electrostatic interactions with CTC, which is negatively charged. This stronger electrostatic attraction contributes to the formation of more stable and stronger complexes between Fe^{3+} and CTC [45]. In summary, based on this comparative study, CTC is more effectively removed by humid Fe/Ca-Alg@K beads. The presence of water within the beads enhances the adsorption process, while the combination of

Fe^{3+} and Ca^{2+} in the alginate hydrogels provides improved adsorption capacity compared to using Ca^{2+} alone.

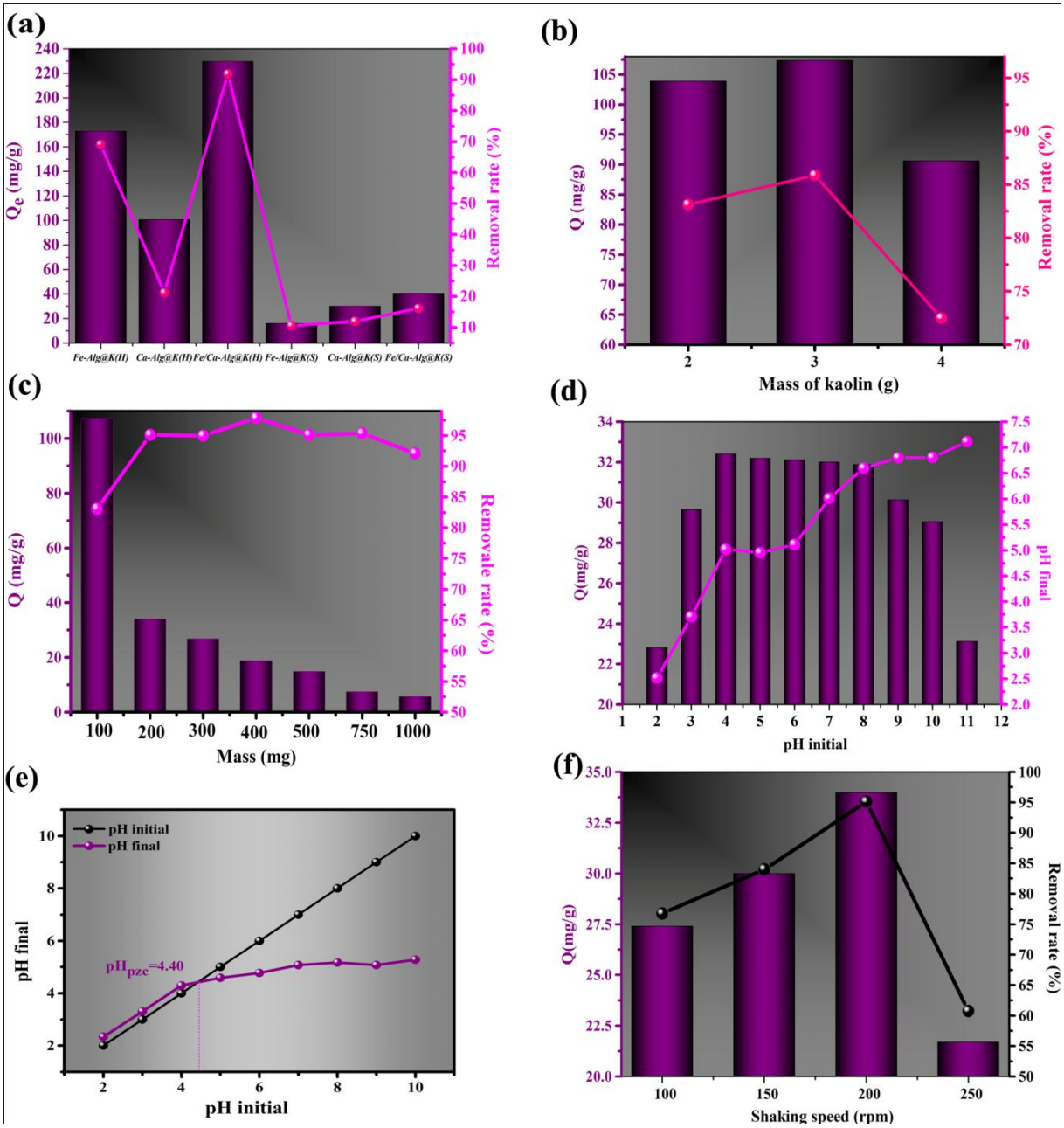


Fig.4 Effect of the (a) physical state of the beads and the type of cross-linkers (T=298K, t=4h, SS=200 rpm, C_0=100 mg/L, $m_{adsorbent}$=100 mg); (b) kaolin dose in alginate beads(T=298K, t=4 h, SS= 200 rpm, m= 100 mg, C_0=50 mg/L); (c) adsorbent dose; (d) pH; and(e) pH_{PZC}(f) shaking speed (T=298K, t=4 h, C_0=50 mg/L, $m_{adsorbent}$=200 mg).

368 *3.2.2. Effect of the kaolin dose in alginate beads*

369 The adsorption process of beads can be significantly influenced by the dosage of clay fillers.
370 **Fig.4b**shows that increasing the amount of K in alginate beads from 2 g (Fe/Ca-Alg@K) to 3
371 g (Fe/Ca-Alg@K-3) results in a slight improvement in both the removal rate and adsorption
372 capacity. Specifically, the removal rate increased from 83.125% to 85.87%, and the
373 adsorption capacity increased from 103.90 mg/g to 107.34 mg/g. This can be attributed to the
374 fact that higher concentrations of clay fillers provide a greater number of active sites for
375 adsorption, allowing for a higher quantity of target compounds to be adsorbed.It also suggests
376 that the filler canact as a structural support to maintain the shape of the hydrogel material
377 during the adsorption process[46]. However, it is noteworthy that further increasing the kaolin
378 dosage to 4 g (Fe/Ca-Alg@K-4)leads to a notable decline in boththe removal rate and
379 adsorption capacity, which decrease to 72.5% and 90.62 mg/g, respectively. This decrease can
380 be attributed to the adverse effects of excessive clay filler doses, such as aggregation and pore
381 blockage within the alginate beads. The aggregation of clay particles reduces the available
382 surface area for adsorption and limits the accessibility of the CTC to the active sites.
383 Additionally, pore blockage hampers the diffusion of CTC into the internal pores of the beads,
384 resulting in reduced adsorption efficiency. Similar findingswere reported in previous work by
385 Reddy, et al., wherethe release rate decreased asfiller concentrationin the polymer
386 matrixincreased.This is due to the enhancedstiffness of polymer chains and reduced
387 microbeadsporosity at higher crosslink densities, which impede the transport of D-
388 Penicillamine (D-PA) through thebeadssurface[47]. An optimized dosage of 3 g ofK was
389 identified as the most effective amount of filler in alginate beads, ensuring the desired
390 adsorption performanceand stable spherical morphology as well (**Fig.S3**). Therefore, Fe/Ca-
391 Alg@K-3 beads were used in the next experiments.

392 *3.2.3.Adsorbent dose effect*

393 The impact of the amount of adsorbent was evaluated by varying it from 100 to 1000 mg for a
394 50 mg/L CTC concentration over 4 h. The findings are illustrated in **Fig. 4c**. The removal rate
395 of CTC increased with the adsorbent dose, peaking at 97.87% with a dose of 400 mg. This
396 suggests that a higher adsorbent dose offers more binding sites for CTC. However, the
397 adsorption capacity significantly decreased, likely due to the surplus of binding sites for CTC
398 adsorption, which enhances the removal rate while lowering the remaining CTC concentration
399 in the solution. This can lead to incomplete utilization of active sites and a reduction in

adsorption per unit weight of adsorbent [46].An optimal adsorbent dose of 200 mg was identified, achieving a maximum adsorption capacity of 33.97 mg/g and a high removal rate of 95.125% for a CTC concentration of 50 mg/L.**Table 2**shows that beads possess the highest removal rate and adsorption capacity compared to K and Fe/Ca-Alg beads, which means that K significantly enhances the loading capacity of CTC by providing more binding sites within the alginate framework.

Table.2 Adsorption capacity and removal rate of CTC on K, Fe/Ca-Alg, and Fe/Ca-Alg@K-3 beads.

	K	**Fe/Ca-Alg**	**Fe/Ca-Alg@K-3**
Q (mg/g)	9.553	28.794	33.973
R (%)	41.382	80.660	95.125

3.2.4.pH effect

The pH effect on the adsorption behavior of Fe/Ca-Alg@K-3 towards CTC wasexamined at a pH range from 2 to 11. As shown in**Fig. 4d**, the highest CTC adsorption and removal rate (%) (32.41 mg/g and 95.12 %) was observed at pH 4-8, followed by a slight decrease as pH increased. CTC species dominated by the solution pH were $CTCH_3^+$, $CTCH_2^{\pm}$, $CTCH^-$, and $CTC^{2-}$when pH < 3.30, 3.30< pH< 7.44, 7.44 < pH < 9.27, and pH > 9.27, respectively[48, 49]. The pH_{PZC} value of Fe/Ca-Alg@K-3 was measured as around 4.40 (**Fig. 4e**).When the pH<pH_{PZC}, the adsorbent surface carries a positive charge, while at pH>pH_{PZC}, it becomes negatively charged. The strong electrostatic repulsion between CTC ($CTCH_3^+$) and the positively charged surface of beads inhibited CTC adsorption, resulting in low adsorption performance. Conversely, in thepH range of 4-8, CTC molecules adoptedneutralcharge, minimizingelectrostatic repulsion.Consequently,the zwitterions species of CTC could interact with negativelycharged adsorbent through electrostatic interaction ($-X^-$ -$CTCH_2^{\pm}$). Thus, the increase in interaction between Fe/Ca-Alg@K-3 beads resulted in a higher adsorption capacity of CTC. On the other hand, despite the potential positive-positive electrostatic repulsion at pH levels below 4 and the negative-negative electrostatic repulsion at pH levels above 8, the removal capacity remained relatively high. It wasnoted that the removalrates were 63%-83% at pH 2-3 and 84.37%-64% at pH 9-11. This suggests that the adsorption of CTC onto composite is not primarily governed by electrostatic interactions. Instead, other

dominant interactions such as hydrogen bonding, complexation, and n-π interactions are likely responsible [25].

It can be observed that when the pH is below 4.00, a high concentration of H^+ ions competes with CTC for adsorption sites on the beads, leading to suppressed CTC adsorption. This observation is supported by the rise in final pH. As the pH of the solution increases, this competition diminishes. Furthermore, the equilibrium pH of the solutions tends to be close to neutral, indicating that the beads possess a certain buffering capacity. In strongly alkaline conditions, the final decrease in pH can be attributed to theOH^- ions compete more effectively than CTC for adsorption sites on the beads.This interaction reduces the concentration of OH^- ions in the solution, further impacting the overall pH [50].

3.2.5.Shaking speedeffect

Agitation is a critical factor in any mass transfer process as it enhances the contact between the adsorbent and the adsorbate, thereby facilitating adsorption. However, in certain cases, agitation can lead to desorption. To investigate the impact of shaking speed (SS) on the adsorption of CTC by beads, testswere conducted while keeping the previously determined optimal parameters constant. Shaking speed wasrangedfrom 100 to 250 rpm. The findings are presented in **Fig. 4f.** For moderate stirring speeds ranging from 100 to 150 rpm, the adsorption of CTC onto the beadswas relatively slow and increased gradually,with corresponding removal rate of 76.75% and 84%, respectively. On the other hand, an agitation speed of 200 rpm exhibited the highest adsorption capacity and a favorable removal rate for an initial CTC concentration of 50 mg/L. At this speed, the maximum adsorption capacity was measured as 33.97 mg/g, with a high removal rate of 95.12%. This speed increases the movement of the solution, which helps CTC molecules to reach the surface of Fe/Ca-Alg@K-3 faster, also CTC molecules move more quickly and evenly throughout the solution, increasing the rate atwhich they come into contact with the beads, thereby facilitating a faster achievement of equilibrium.Without enough agitation (100 to 150 rpm), the corresponding removal rates were 76.75% and 84%, respectively.This can be explained by the fact that CTC molecules might remain in the solution longer, resulting in a slower adsorption process. However, at a speed of 250 rpm, the adsorption capacity and removal rate of CTC decreased to 21.69 mg/g and 60.75%, respectively, due to a decrease in diffusion speeds.

This may happen because the high shaking speed supplied enough additional energy to disrupt the newly formed bonds between CTC and the adsorbent surface. This phenomenon, known

as swirling, led to the desorption of CTC [51, 52].It has been reported previously that adsorption increases with rising agitation speeds only up to a certain limit, beyond which there is no significant increase in adsorption capacity[53].

3.2.6.Contact time effect

Fig. 5adepicts the adsorption behavior of CTC on Fe/Ca-Alg@K-3.At first,adsorption occurs quickly, showing higher capacities at lower concentrations:4.37mg/g for 25 mg/L and 15.80 mg/g for 50 mg/L. As time passes,the adsorption capacity slowly increases and thenstabilizes at 15.27 mg/g and at 30.67 mg/grespectively after 180 min. The beads achieved equilibrium in just 180 min, suggestingthat the higher concentration of CTCin the solution (50 mg/L) enhances mass transfer.The sufficient availability of adsorption sites ensures a high probability of collision between CTC molecules and the beads,facilitating more rapid adsorption rate. After the composite beadsrapidly adsorbed a huge amount of CTC at 180 min, many adsorption sites became occupied, leading to a decline in the adsorption rate.Therefore, based on these findings, the optimal contact time for CTC removal by the beads was 180min. The adsorption equilibrium reached in this study exceeds the rates documented for other adsorbents, including a rubber waste-derived polymer composites (300 min) [54], Co-doped 3D petal-like ZnIn2S4/GaN(320 min) [55], as well shrimp shell waste(2160 min)[56].

3.2.7. Effect of initial CTC concentration

To examine the influence of the adsorbate on adsorption behavior, various concentrations of CTC were utilized (10, 20, 30, 40, 50, 75, 100, 125, 150, 175, and 200 mg/L, respectively). **Fig. 5b**displays the initial concentration effectof CTC,with values ranging from 6.02 to 95.12 mg/g, 6.78 to 112.09 mg/g, 3.97 to 117.76 mg/g, and 5.98 to 84.91 mg/g at 298, 308, 318, and 328K, respectively. The maximum uptake capacity (Q_{max}) was significantly influenced by the CTC concentration, with Q_{max} values increasing proportionally as the concentration increases.These findingscan be explained by the equilibrium between the CTC moleculesand the activesites on the Fe/Ca-Alg@K-3;as the number of adsorbate molecules gradually increased,the saturation of the adsorption sites happenedmoreswiftly.Comparable results were notedby Da Silva Bruckmann et al. [57] and Nasiri et al. [58] when removing tetracycline using graphene oxide modified Fe_3O_4 and $CuCoFe_2O_4$@Chitosan.

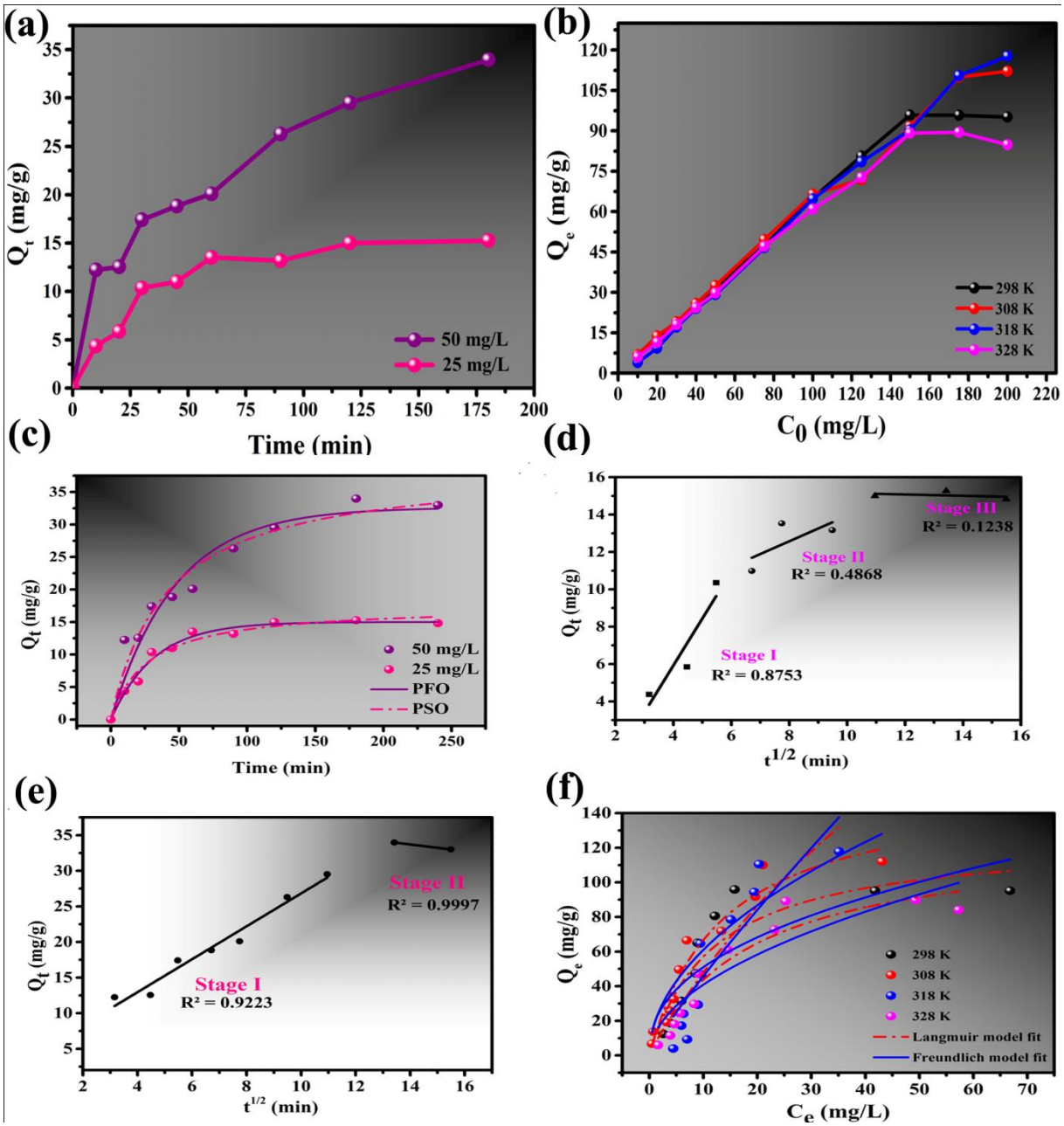


Fig.5 (a) Effect of time for CTC adsorption on Fe/Ca-Alg@K-3 with two initial CTC concentrations (25 and 50 mg/L); (b) Initial concentration effect on the adsorption capacity of CTC; (c) PFO and PSO kinetics models for CTC adsorption on Fe/Ca-Alg@K-3; (d-e) IPDmodelfor CTCadsorption(at 25 and50 mg/L, respectively);and (f) The fitting of Langmuir and Freundlich isotherms on CTC adsorption by Fe/Ca-Alg@K-3 at temperatures of 298, 308, 318, and 328K.

3.2.8. Adsorption Kinetics

To gain a clearer understanding of the adsorption process, PFO and PSO kinetic models were used to describe the adsorption kinetics of CTC onto the studied beads **(Fig. 5c)**. The

PFOmodel indicates that the removal process carried out in a single step, while the PSOmodel assumes that the adsorption process involves multiple steps and is considered a more complex mechanism.To determine the appropriatekinetic model that aligns withthe experimental data, two primary criteria must be considered:The R^2 value of the appropriate kinetic model should exceed that of the other models used, and there should be a correlation between Q_{exp} and Q_{cal} from the suitable model. Accordingly, both models exhibited higher R^2 values (> 0.93) **(Table 3)**. This reveals that the remediation process is governed by both chemical and physical adsorption mechanisms. Similar trend has been observed by Douba et al. during the removal of malachite green using Ca-ALG@MCM-41 composites beads [RefDouba 2025]. Furthermore, the calculated Q_e values from the PFOmodel align better with the experimental values, indicating that physisorption is the dominant mechanism [33]. The adsorption of CTC onto the beads was likely affectedby two factors: (1) external mass transfer of CTC molecules from bulk solution to the bead's outer surface, followed by (2) diffusion into the bead's internal pores (intraparticle diffusion). To evaluate the role of diffusion in the adsorptionbehavior, the kinetic data were analyzed using the intraparticle diffusion (IPD) model [59]. This modeling approach was designed to elucidate the impact of diffusion on the overall adsorption behavior.For a concentration of 25 mg/L, the adsorption curves of the Fe/Ca-Alg@K-3displayed three linear regions (**Fig. 5d**), suggesting a triphasic removal mechanism involving: (i) rapid surface adsorption, (ii) gradual pore diffusion, and (iii) final equilibrium stabilization.The internal diffusion rate constants were ranked as K1d > K2d > K3d. Moreover, the intercept values of the fitting curves (C1, C2, and C3) were all greater than zero, ranging from 4.119 to 15.492 (**Table.3**), suggesting that intra-particle diffusion was not the rate-limiting factor. As for 50 mg/L, the adsorption curve exhibited two distinct linear ranges. In summary,kinetic data demonstrates that CTC removal on the beads proceeds via two distinct regimes: (1) rapid surface film diffusion dominates the initial removal phase, while (2) pore diffusiondetermines the overall rate-limiting behavior [50].

Table.3 Kinetic parameters for CTC removal onto Fe/Ca-Alg@K-3.

Kinetic models	Parameters	Initial CTC concentration	
		25 mg/L	50 mg/L
Pseudo-first-order	$Q_{e(exp)}$ (mg/g)	15.800	30.670
	$Q_{e(cal)}$ (mg/g)	15.011	32.260
	K_1 （1/min）	0.031	0.021
	R^2	0.978	0.931
Pseudo-second-order	$Q_{e(cal)}$ (mg/g)	17.562	38.974
	K_2 （g/mg.min）	0.002	6.284
	R^2	0.976	0.956
Weber-Morris intraparticle diffusion	K_{1d} (mg/g.min ½)	2.512	2.312
	C_1(mg/g)	4.119	3.699
	R_1^2	0.875	0.922
	K_{2d} (mg/g.min ½)	0.684	0.851
	C_2 (mg/g)	7.096	4.071
	R_2^2	0.486	0.999
	K_{3d} (mg/g.min ½)	0.034	
	C_3 (mg/g)	15.492	
	R_3^2	0.123	

3.2.9. Adsorption isotherm

To interpret the nature of the interaction between CTC and composite beads, the experimental data were comprehensively analysed by Langmuir and Freundlich isotherm models **(Fig. 5f)**.The values of R^2 were in the range of 0.836-0.941, while the values of the adsorption capacities [$Q_{e(cal)}$ (mg/g)] were in the range of 125.786-156.468. This suggests that the Langmuir model provides a more accurate representation of the isotherm data, with a CTC uptakecapacity of 156.468 mg/g at 308 K and a high R^2 (0.941). The Langmuir isotherms indicate that adsorption takes place on a homogeneous surface, with adsorbate forming

monolayers on the adsorbent surfaces. In the Langmuir model, K_L is a key parameter that demonstrates the affinity of the binding sites. If K_L is between 0−1, the adsorption of CTC onto composite beads is deemed favourable [50], as observed in **Table.4**. Interestingly, the values of 1/n (<1) and RL (ranging between 0 and 1), indicated that the adsorption of CTC onto composite beads was favourable [25]. This further supports the effectiveness and favorable nature of the adsorption process under the studied conditions.

It is noticeable that adsorption is influenced by temperature, especially at higher concentrations. An increase in temperature results in a slight increase in the maximum adsorption capacity. This is attributed to the elevated reaction temperature, which accelerates the movement of CTC molecules, thereby increasing the collision frequency [60]. However, further increases in temperature can lead to a decrease in adsorption equilibrium. This decline may be due to changes in the stability of the adsorbate-adsorbent interactions or potential desorption effects that can occur at higher thermal energies. Consequently, while moderate temperature increases can enhance adsorption, excessive temperatures may negatively impact the overall adsorption efficiency.

Table.5 summarizes a comparison of this research with previously reported literature data, highlighting that the composite beads demonstrated effective sorption performance for CTC. The results demonstrate that the beads exhibits significantly higher CTC uptake capacity than most other listed adsorbents, demonstrating their superior performance in removing CTC compared to other adsorbents. Therefore, composite beads are considered an effective and promising candidate for the removal of pollutants from wastewater.

570 **Table.4** Parameters of the isotherm models for chlortetracycline adsorption by Fe/Ca-
571 Alg@K-3.

Isotherm models	Parameters	Temperature			
		298 K	**308 K**	**318 K**	**328 K**
Langmuir	$Q_{e(exp)}$ (mg/g)	95.120	112.090	117.760	84.910
	$Q_{e(cal)}$ (mg/g)	125.813	156.468	137.115	125.786
	K_L （L/mg）	0.082	0.074	0.012	0.053
	R^2	0.836	0.941	0.823	0.918
	R_L	0.006-0.549	0.063-0.575	0.039-0.890	0.278-0.654
Freundlich	$1/n_F$	0.420	0.507	0.876	0.511
	K_F $(mg/g)(L/mg)^{1/n}$	19.384	18.943	6.092	12.600
	R^2	0.687	0.887	0.799	0.830

572

573 **Table.5** Comparative evaluation of CTC uptake capacities across different adsorbents.

Adsorbent	pH	Time (min)	Q_{max} (mg/g)	Reference
Magnetic peanut shells	5	60	82.96	[61]
Chitin	7	120	12.01	[62]
La-zeolite[a]	7	20	127.55	[63]
ball-milled biochar	7	180	39.10	[64]
Ws-L biochar[b]	7	-	31.48	[65]
La@SA/CMC-MMT-0.5[c]	7	300	109.12	[38]
PVDF/PANI/MT[d]	6	1440	51.00	[66]
Fe/Ca-Alg@K-3	4-7	180	156.468	**This study**

574 [a]lanthanum modified zeolite, [b]Lignin impregnated wheat straw biochar, [c]La@SA/sodium carboxymethyl
575 cellulose-montmorillonite(MMT),and [d]poly(vinylidene fluoride)/polyaniline-MMT.

576

577

3.2.10. Thermodynamic study

The thermodynamic parameters for the adsorption of CTC on the beads were assessed using the Plot of LnK_d vs 1/T (**Fig.S4)**.**Table.6**lists the determined thermodynamic parameters. The value of ΔH° for CTC adsorbed by the beads is -14,082 kJ/mol, which indicates the favourability of physi-sorption.The negative value of ΔH° less than -20 kJ/mol suggests that the adsorption process is exothermic and is likely to be physisorption [67, 68]. During the adsorption process, an increase in the system's temperature causes a decrease in CTC adsorption; therefore, chemical adsorption is unlikely in this system.

The uptake of CTC was found to be spontaneous and highly favorable across all temperatures (ΔG°<0). Furthermore, the reduction in ΔG° with increasing temperature indicates that the process becomes thermodynamically unfavorable at higher temperatures [58]. Typically, ΔG° values below -20 kJ/mol are associated with electrostatic interactions between charged molecules and the charged adsorbent (physisorption). When the mean free energy drops below -40 kJ/mol, it implies that charge sharing or transfer occurs from the adsorbate to the beadssurface, leading to the formation of coordinate bonds (chemisorption) [69]. The ΔG° values are below -20 kJ/mol, confirming physisorption. Additionally, the negative ΔS° value (-32.881 J/mol·K) indicates a more ordered arrangement of CTC on the surface of the beads after adsorption, reflecting a decrease in randomness at the solid/solution interface [70].

Table.6 Thermodynamic parameters.

Temperature (K)	ΔG° (kJ/mol)	ΔH° (kJ/mol)	ΔS° (J/mol. K)
298	-4.284		
308	-3.955	-14.082	-32.881
318	-3.626		
328	-3.297		

2.3. Effect of co-existing ions

The composition of real water bodies is quite complex, with organic pollutants coexisting alongside various substances, including inorganic ions. Therefore, it is crucial to investigate the effects of these coexisting substances on the removal of CTC by Fe/Ca-Alg@K-3

composites for practical applications. Inorganic salts such as KCl, $CaCl_2$, Na_2SO_4, and KNO_3 are used to study the effects of co-existing ions on removal capacities. **Fig.6a** shows that the presence of different studied ions inhibited the adsorption of CTC, following the order: SO_4^{2-} < NO_3^-< Cl^- < Ca^{2+}. The existence of SO_4^{2-} and NO_3^-ions slightly inhibited the removal efficiency of Fe/Ca-Alg@K-3 due to its resistance to these anions, thus enhancingelectrostatic repulsion between the composite beads andthe competing anions(SO_4^{2-}/NO_3^-) in solution.However,the removal of CTC on Fe/Ca-Alg@K-3 beads decreased to 79% in the presence of Cl ions because Cl^- ions can form complexes with metal ions (e.g., Fe^{3+} or Ca^{2+}) in the adsorbent, reducing their availability for interactions with CTC. In addition, if the surface of the material becomes negatively charged in the presence of Cl^- ions, it may repel the negatively charged functional groups of CTC (e.g., deprotonated hydroxyl or carboxyl groups), reducing adsorption efficiency [71]. On another hand, the addition of Ca^{2+} ions significantly reduced the adsorption capacity of CTC to 75%.The presence of co-existing cations facilitates both (i) cationic bridge formation, and (ii) soluble cation-antibiotic complexation, collectively altering adsorption behavior [72].In addition, since cation exchange with Ca^{2+} or Fe^{3+} may involve in the mechanism of CTC adsorption on the studied beads, the introduction of a second cation into the system is anticipated to reduce CTC adsorption due to competitive effects. Typically, the concentrations of Na^+, Ca^{2+}, and Mg^{2+} are below 100 mg/L, which is less than 0.001 mol/L. Consequently, the presence of these coexisting cations is unlikely to affect CTC adsorption on the beads in practical applications [25].

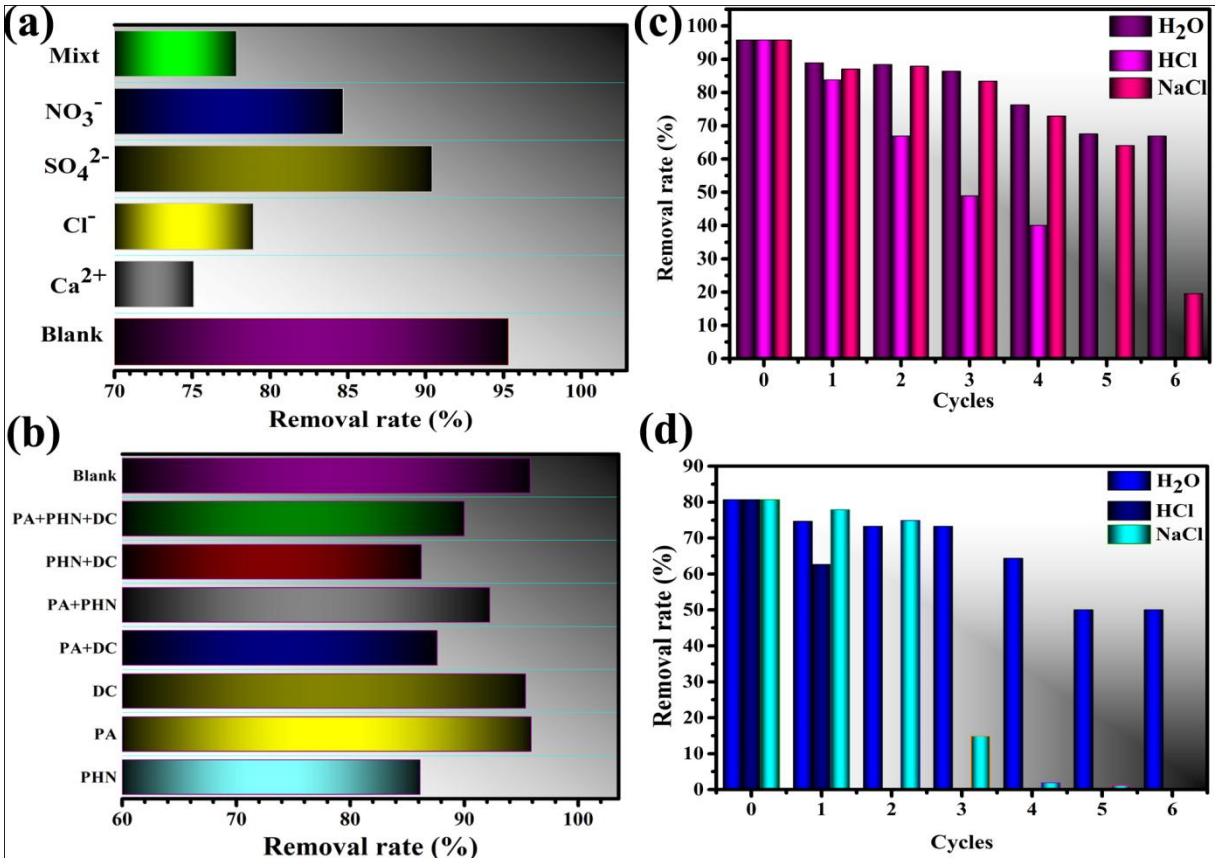


Fig.6(a) Effect of co-ions on the removal rate of CTC on Fe/Ca-Alg@K-3;(b) effect of co-existing organic compound on the removal rate of CTC on Fe/Ca-Alg@K-3; and regeneration study of (c) Fe/Ca-Alg@K-3 beads and (d) Alg beads.

2.4. Effect of co-existing organic compounds

Co-existing organic substancesin aquatic environments may affect the CTC adsorption. Adsorption of CTC on the beadsin the presence of phenoxymethylpenicillin (PHN), paracetamol (PA), or diclofenac sodium (DC) was studied **(Fig. 6b)**. The removal efficiency of CTC was not affected by the presence of PA and DC in water. However, it decreased by approximately 10% in the presence of phenoxymethylpenicillin because it could bond more firmly with the beads compared to other studied organic compounds. However, the removal rate is still above 85 % which means that the studied adsorbent possesses a good selectivity toward CTC and hasa more binding site that could adsorb more organic pollutants. Previous studies found similar results [38, 73].

2.5. Reusability studies

The regeneration of depleted adsorbents was demonstrated by eluting them with various eluents (**Fig. 6c-d**). To identify the most suitable eluent for desorbing CTC, three eluents (DW, 0.1 M NaCl, and 0.1 M HCl) were chosen as desorption solutions to assess composites effectiveness reusability.**Fig. 6c** shows the recovery of Fe/Ca-Alg@K-3 beads. In the first cycle, the CTC removal efficiencies of composites were slightly decreased compared to those of the original Fe/Ca-Alg@K-3 (95.125 %). By the fifth cycle, the removal efficiency reduced to 67.5%, 0%, and 64% for the water, HCl, and NaCl desorption solutions, respectively. This suggests that a considerable number of the adsorption sites were irreversible and not accessible. After 5 cycles, the removal rate of the beads remained at 66.87 %with the waterdesorption solution, indicating that the beads can be effectively recycledmultiple times.It was also shown that the active binding sites on the beads could be effectively regenerated.Conversely,the alginate beads demonstrated lowreusability (**Fig. 6d**). This highlights that K greatly improved the adsorbent's reusability. The study confirmed thatH_2O is the most effective eluent for CTC desorption. Additionally, the beads achieved a higher CTC removal efficiency compared to alginate beads, with an improvement of around 11%. This suggests that CTC was successfully adsorbed not only onto the alginate matrix but also onto the K minerals surfaces in the beads.FT-IR spectrum of the regenerated Fe/Ca-Alg@K-3 **(Fig. S5)** was in good agreement with that of the synthesized composites, suggesting that the structure of the material was well preserved during the recycling experiment.

2.6. Application of the beads in the real pharmaceutical and surface wastewaters spiked CTC

Encouraged by the results described above, the removal rate of CTC from pharmaceutical and surface wastewaters using Fe/Ca-Alg@K-3 was investigated, in which the CTC at a concentration of about 50 and 100 mg/L was intentionally added **(Fig. 7a-b)**. Time-course adsorption measurements showed that the beads can efficiently remove CTC from wastewater at a contact time of 3 h, where the removal rate achieved 79 % in both samples, even at higher concentrations using 500 mg of the beads. Therefore, the beads efficiently capture CTC from original wastewaters samples with both low and high concentrations,despite the presence of a large number of competing ions and organic compounds.

2.7. Application of the beads in the real pharmaceutical wastewaters

The results underscored the considerable potential of Fe/Ca-Alg@K-3 for decontaminating wastewater containing CTC. However, it is crucial to recognize that actual polluted water often contains a diverse array of ions, including Ca^{2+}, Na^{+},Mg^{2+}, NH_4^{+}, SO_4^{2-}, CO_3^{2-},NO_3^{-}, and Cl^{-}, as well as a diverse range of organic compounds (such as antibiotics, phenols, etc.), which can increase the COD concentration. It is an important parameter used to assess the quality of water bodies and the effectiveness of wastewater treatment processes [74]. To assess the practical applicability of the composites, the study utilized pharmaceutical wastewaters. The results presented in **Fig. 7c** demonstrated a notable decrease in the residual COD concentration in the wastewater. Specifically, the COD decreased from an initial 292,8 mg/L to 170 mg/L, 100,8 mg/L, and 52,8 mg/L after the addition of 100 mg, 200 mg, and 500 mg of the composites, respectively. These levels were found to meet the allowable COD discharge standards. Furthermore, the data indicate that a dosage of 200 mg of the adsorbent was sufficient to reduce the COD concentration to permissible limits (<120 mg/L) [75].

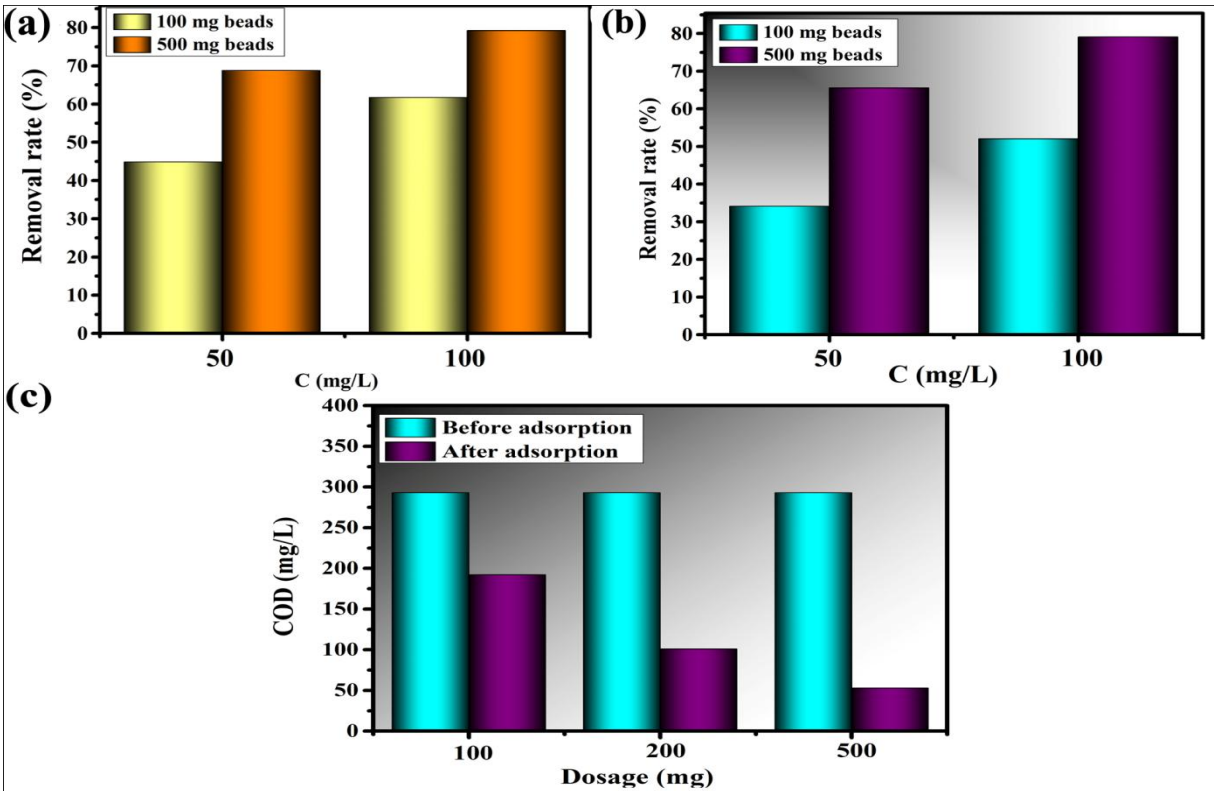


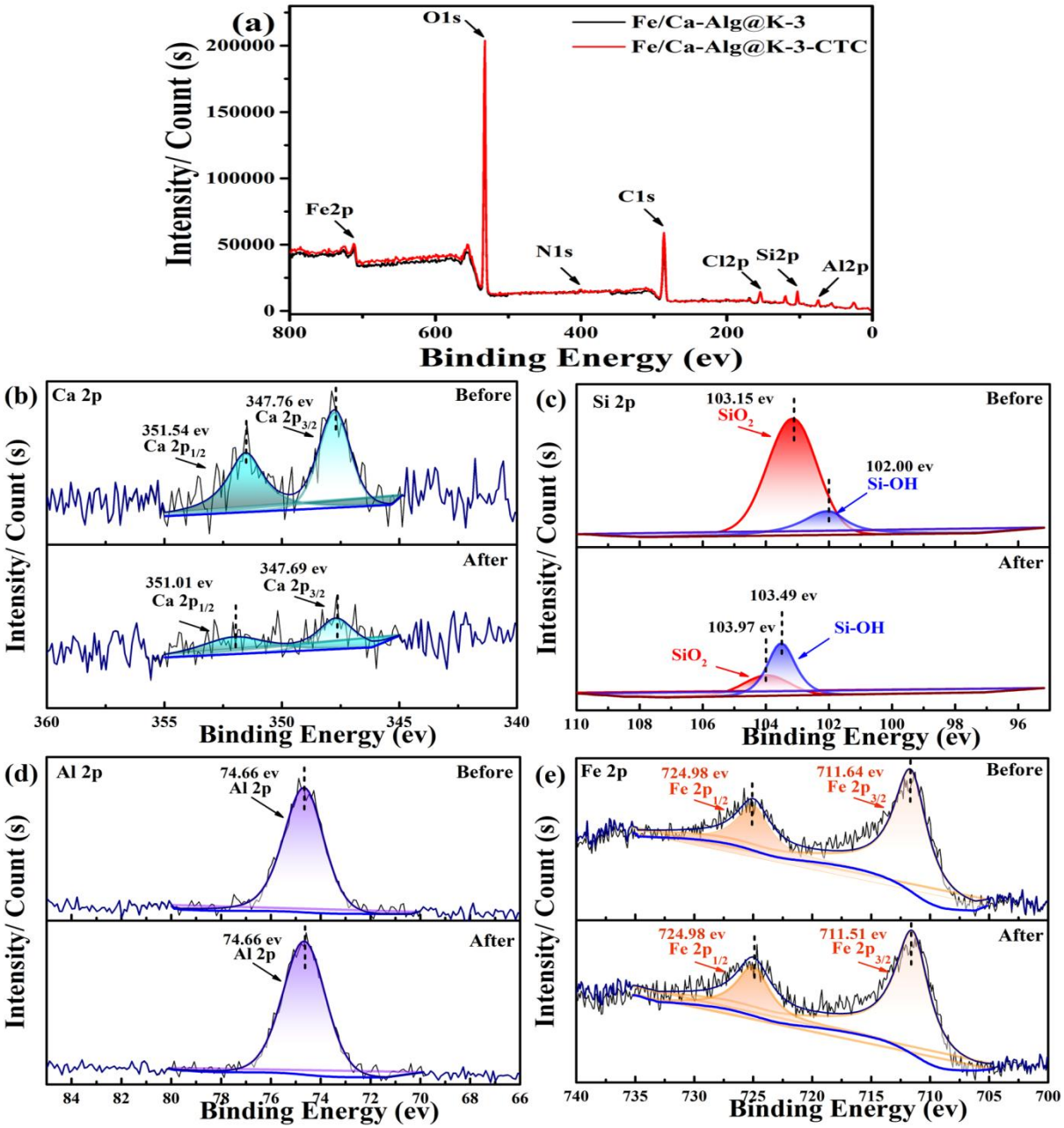
Fig.7 Chlortetracyclinehydrochloride removal in pharmaceutical (a) and surface wastewater (b) spiked CTC at different dosages of the Fe/Ca-Alg@K-3; and (c) COD removal of the beads in the real pharmaceutical wastewaters.

2.8. XPS analysis for mechanism of CTC adsorption

In the context of studying the mechanism of CTC adsorption, XPS can provide valuable insights into the interactions between CTC and the adsorbent material. **Fig. 8** depicts the high-resolution XPS spectra of thebeads, both prior to andafter adsorption.The survey XPS spectra (**Fig. 8a**) indicated that the primary elements of Fe/Ca-Alg@K-3 were C, N, O, Al, Si, Fe, and Ca. After the adsorption of CTC, a characteristic peak emerged near 400 eV in the XPS spectrum of the composite beads (**Fig. 8a**), which could be assigned to the N 1s peak [76]. This observation suggests that CTC was effectively immobilized on the surface of the beads. The peak intensity of C and O also increased after CTC adsorption, further indicating the adsorption process [77]. To explore the adsorption mechanism of CTC by the prepared beads, the changes in Ca, Al, Fe, and Si elements before and after CTC adsorption were investigated. The results displayed that following the adsorption of CTC, the characteristic peak corresponding to $Ca2p_{3/2}$ and $Ca2p_{1/2}$shifted from 347.76 to 347.69eV and from 351.54 to 352.01 eV (**Fig. 8b**), indicating that hydroxyl (-OH) groups and a keto group (C=O) in CTC might interact chemically with calcium ions, potentially forming a complex or precipitate. This interaction may alter the electronic environment of the calcium, leading to the decrease in intensity of its XPS peak. Moreover, the hydroxyl, carbonyl, and amino groups present within the CTC molecules donated a substantial quantity of electrons to Ca, facilitating the creation of metal complexes with Ca(II) via cation-π and cation-n bonding interactions [77, 78]. Another possible mechanism is the cation exchange mechanism between Ca^{2+} and CTC [25]. This exchange has been identified as a key mechanism in the interaction between clay-based adsorbents and tetracyclines. Evidence supporting this includes the observation of desorbed metal cations, including Ca^{2+}, which originate from clays or clay-alginate composites[79]. In **Fig. 8c**, the characteristic peaks of Si 2p at 102.00 eV and 103.15 eV, corresponding to Si-O and SiO_2 groups [49], show a significant positive shift in binding energy (from 103.15 eV to 103.97 eV) after CTC adsorption. This shift suggests the formation of a silanol bond between SiO_2 and –H groups of CTC. The increased intensity and shift (from 102.00 eV to 103.49 eV) of the Si-OH peak further confirm hydrogen bonding between SiO_2 on Fe/Ca-Alg@K-3 and the –H groups of CTC molecules. Additionally, other possible mechanisms include electrostatic interactions between $Si\text{-}O^-$ and CTC^+, as well as cation-n and cation-π interactions involving Si^{4+} and CTC. In **Fig. 8d**, the characteristics peak of Al 2p was observed at 74.66 eV [80]. No shifting of binding energy was observed after CTC adsorption, indication that Al did not participate in the adsorption process. In the Fe 2p

721 spectrum of Fe/Ca-Alg@K3 (**Fig. 8e**), the peaks at 711.64 and 724.98 eV were assigned to Fe
722 2p3/2 and Fe2p1/2spin-orbit splitting, respectively [81]. The characteristic Fe 2p3/2 peak
723 shifted by approximately 0.13 eV after CTC adsorption, suggesting that Fe (III) might also
724 participate in complex formation with CTC via cation-n and cation-π bonding bridges.

725 The proposed mechanism of CTC adsorption isillustrated in **Fig.9.** Based on the
726 characterization results, pH effect, adsorption kinetics, and isotherm analyses, the adsorption
727 of CTC onto the beads appears to be governed by a combination of chemical and physical
728 interactions, along with the surface uniformity of the composite beads. Moreover, calcium and
729 iron in Fe/Ca-cross-linked SA, K encapsulated in the beads, and Fe/Ca that may bound to K
730 minerals were the three potential adsorption sites in Fe/Ca-cross-linked Alg@K-3 beads. The
731 mechanism for CTC removal might involve strong n-π EDA interactions and hydrogen
732 bonding between the active oxygen on Fe/Ca-Alg@K-3 and CTC molecules. Additionally,
733 the cation-n and cation-π bonding bridges between CTC and Fe/Ca cross-linkedAlg@K-3,
734 along with hydrogen bonding, electrostatic interactions, cation exchange, and the diffusion of
735 CTC into the pores of the beads, all contribute to the adsorption process.



736

737 **Fig. 8**(a) XPS surveyspectra of Fe/Ca-Alg@K-3 beads before and after CTCremoval and

738 High-resolution XPS spectra of (b) Ca 2p, (c) Si 2p, (d) Al 2p, and (e) Fe 2p.

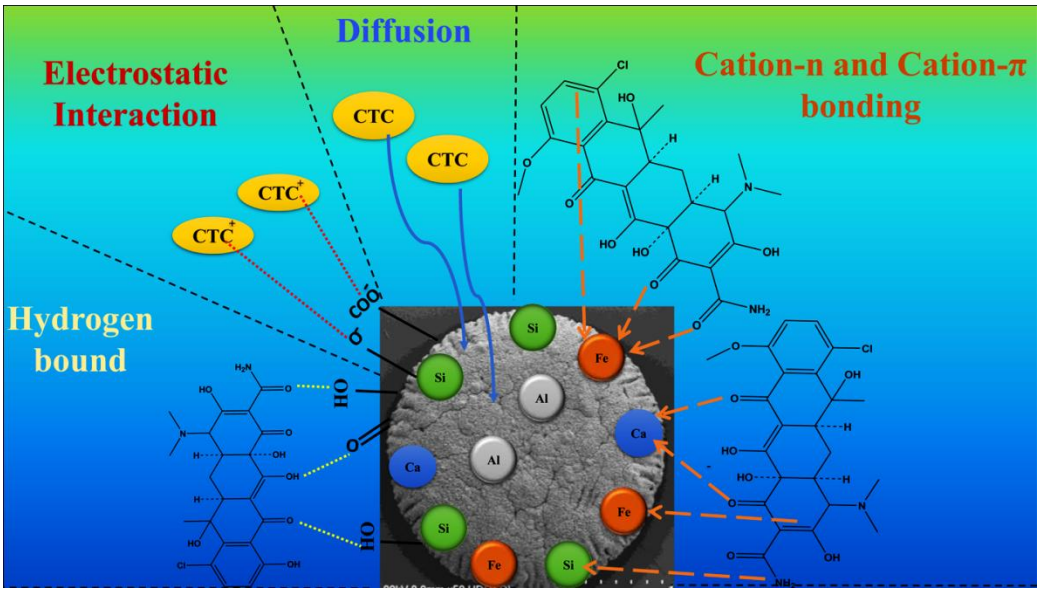


Fig.9 Proposed interaction mechanism of CTC on Fe/Ca-Alg@K-3.

3. Conclusion

In this research,dual cation cross-linked alginate-kaolin hydrogel beads were synthesized for the removal of CTC. The SEM analysis showed that the beadspossess an irregular microstructure made up of polyhedral particles of different sizes,while FT-IRconfirmed the successful formation of composites and the adsorption of CTC. Batch experiment studies revealed that an optimal dose of 200 mg Fe/Ca-Alg@K was efficient in CTCremoval,achieving a higher CTC uptake capacity of 30.67 mg/g and an efficient removal rate of 95.12% for an initial CTC concentration of 50 mg/L within 3 hat a shaking speed of 200 rpm.The pH studies showed that the adsorbent could effectively remove CTC in the pH range from 4 to 8, suggesting that electrostatic interactions do not primarily govern the adsorption process.Instead, other dominant interactions, such as hydrogen bonding, complexation, and n-π interactions, play a significant role. The PFO and PSO models closely align with the experimental data, demonstrating that both models fit well.Modelling of the CTC adsorption isotherms revealed that the Langmuir model, with a high R^2 (0.94%) and a CTC maximum uptake capacity (156.46 mg/g at 318K), suggests homogeneous adsorption and monolayer formation, indicating that the adsorption process for CTC was favorable. Fe/Ca-Alg@K beads exhibited high selectivityfor CTC from complex water matrices. Regeneration studies revealed the reusability of Fe/Ca-Alg@K beads, emphasizing their enhanced ability for recyclability due to K incorporation.The adsorption process of CTC was favorable and spontaneous process at room temperature. Additionally, the adsorption process

is exothermic.COD study indicates that 200 mg of beads was sufficient to reduce the COD concentration in pharmaceutical wastewaters to the permissible limits of less than 120 mg/L. The application of Fe/Ca-Alg@K beads in real wastewatersdemonstrated efficient capture of CTC from both low and high concentration samples, including pharmaceutical and surface wastewaters, despite the presence of a large number of competing ions and organic compounds.

Acknowledgements

This study received funding from PRIMA2/CICLICA, a program backed by the European Union(Project ID 1727) anda Scientific Research Fund of Zhejiang Provincial Education Department(Y202456477).

Declaration of interest

All authors declare thatthey have no competing interests.

References

[1] Singh R, Singh AP, Kumar S, Giri BS, Kim K-H. Antibiotic resistance in major rivers in the world: a systematic review on occurrence, emergence, and management strategies. Journal of Cleaner Production 2019;234:1484-505.

[2] Duggar B. Aureomycin: a product of the continuing search for new antibiotics. Annals of the New York Academy of Sciences 2011;1241:163-9.

[3] Grossman TH. Tetracycline antibiotics and resistance. Cold Spring Harbor perspectives in medicine 2016;6:a025387.

[4] Yuan L, Yan M, Huang Z, He K, Zeng G, Chen A, et al. Influences of pH and metal ions on the interactions of oxytetracycline onto nano-hydroxyapatite and their co-adsorption behavior in aqueous solution. Journal of Colloid and Interface Science 2019;541:101-13.

[5] Mehrjouei M, Müller S, Möller D. Energy consumption of three different advanced oxidation methods for water treatment: a cost-effectiveness study. Journal of Cleaner Production 2014;65:178-83.

[6] Homem V, Santos L. Degradation and removal methods of antibiotics from aqueous matrices–a review. Journal of environmental management 2011;92:2304-47.

[7] Öztürk Er E. Graphene Oxide as a Highly Efficient and Reusable Adsorbent for Simultaneous Removal of Parabens: Optimization by Response Surface Methodology, Adsorption Isotherms and Reusability Studies. Adsorption 2025;31:24.

[8] Aksu Z, Tunç Ö. Application of biosorption for penicillin G removal: comparison with activated carbon. Process biochemistry 2005;40:831-47.
[9] Benahdach K, Ali YAEH, Azzouz A, González MdMC, Chraka A, El Mail R, et al. Synthesis of activated carbon by microwave-assisted sulfuric acid activation for the adsorption of Congo Red in aqueous medium: Kinetic, isotherm, thermodynamic, molecular dynamic, and functional theory studies. Journal of Molecular Liquids 2025;420:126821.
[10] Ahamad Z, Mashkoor F, Nasar A, Jeong C. Multi-walled carbon nanotubes/TiO2/Chitosan nanocomposite for efficient removal of malachite green dye from aqueous system: A comprehensive experimental and theoretical investigation. International Journal of Biological Macromolecules 2025;295:139461.
[11] Alsaheb Z, Hummadi KK. Adsorption of Magnesium Oxide Onto Bentonite for the Purpose of Amoxicillin Elimination from Aqueous Solutions. Available at SSRN 5128734.
[12] Fakhri A, Behrouz S. Comparison studies of adsorption properties of MgO nanoparticles and ZnO–MgO nanocomposites for linezolid antibiotic removal from aqueous solution using response surface methodology. Process Safety and Environmental Protection 2015;94:37-43.
[13] Kamiyango M, Masamba W, Sajidu S, Fabiano E. Phosphate removal from aqueous solutions using kaolinite obtained from Linthipe, Malawi. Physics and Chemistry of the Earth, Parts A/B/C 2009;34:850-6.
[14] Almasri DA, Saleh NB, Atieh MA, McKay G, Ahzi S. Adsorption of phosphate on iron oxide doped halloysite nanotubes. Scientific Reports 2019;9:3232.
[15] Kumar IA, Viswanathan N. Fabrication of zirconium (IV) cross-linked alginate/kaolin hybrid beads for nitrate and phosphate retention. Arabian Journal of Chemistry 2020;13:4111-25.
[16] Awad ME, López-Galindo A, Setti M, El-Rahmany MM, Iborra CV. Kaolinite in pharmaceutics and biomedicine. International Journal of Pharmaceutics 2017;533:34-48.
[17] Murray HH. Kaolin applications. Developments in clay science 2006;2:85-109.
[18] Mustapha S, Ndamitso M, Abdulkareem A, Tijani J, Mohammed A, Shuaib D. Potential of using kaolin as a natural adsorbent for the removal of pollutants from tannery wastewater. Heliyon 2019;5:e02923.
[19] Mustapha S, Tijani J, Ndamitso M, Abdulkareem A, Shuaib D, Mohammed A. Adsorptive removal of pollutants from industrial wastewater using mesoporous kaolin and kaolin/TiO2 nanoadsorbents. Environmental Nanotechnology, Monitoring & Management 2021;15:100414.

[20] Zhao Y, Geng J, Wang X, Gu X, Gao S. Tetracycline adsorption on kaolinite: pH, metal cations and humic acid effects. Ecotoxicology 2011;20:1141-7.
[21] Zhao Y, Gu X, Li S, Han R, Wang G. Insights into tetracycline adsorption onto kaolinite and montmorillonite: experiments and modeling. Environmental Science and Pollution Research 2015;22:17031-40.
[22] Tordi P, Ridi F, Samorì P, Bonini M. Cation-Alginate Complexes and Their Hydrogels: A Powerful Toolkit for the Development of Next-Generation Sustainable Functional Materials. Advanced Functional Materials 2024:2416390.
[23] Zhang X, Lin X, He Y, Chen Y, Luo X, Shang R. Study on adsorption of tetracycline by Cu-immobilized alginate adsorbent from water environment. International journal of biological macromolecules 2019;124:418-28.
[24] Fizir M, Touil S, Richa A, Wei L, Douadia S, Taibi R, et al. Kaolin-iron cross-linked alginate beads for efficient phosphate removal from water: An initiation towards sustainable treatment of domestic and hydroponic wastewaters. Applied Clay Science 2024;256:107430.
[25] Chang P-H, Mukhopadhyay R, Sarkar B, Mei Y-C, Hsu C-H, Tzou Y-M. Insight and mechanisms of tetracycline adsorption on sodium alginate/montmorillonite composite beads. Applied Clay Science 2023;245:107127.
[26] Bai T, Zhao K, Gao Q, Qi M, Zhang Y, Lu Z, et al. Kaolin/CaAlg hydrogel thin membrane with controlled thickness, high mechanical strength, and good repetitive adsorption performance for dyes. Industrial & Engineering Chemistry Research 2020;59:4958-67.
[27] Čejka J, Roth W, Opanasenko M. Two-dimensional silica-based inorganic networks. 2017.
[28] Rouhani M, Ashrafi SD, Taghavi K, Joubani MN, Jaafari J. Evaluation of tetracycline removal by adsorption method using magnetic iron oxide nanoparticles (Fe3O4) and clinoptilolite from aqueous solutions. Journal of Molecular Liquids 2022;356:119040.
[29] Yang J, Du Y, Li W, Shan S, Hu T, Su H. Iron oxide/alginate hydrogel composites for removal of tetracycline via adsorption-coupled Fenton-like reaction. Materials Chemistry and Physics 2024;315:129034.
[30] Hu Y, Pan C, Zheng X, Liu S, Hu F, Xu L, et al. Removal of ciprofloxacin with aluminum-pillared kaolin sodium alginate beads (CA-Al-KABs): Kinetics, isotherms, and BBD model. Water 2020;12:905.
[31] Fizir M, Richa A, Touil S, Fermous R, Tahir C, Hassene I, et al. Comparing Adsorption Properties of Algerian Kaolinite Towards Phosphate with Those of Activated Carbon:

Adsorption Experiments, Molecular Modeling and an Initiative Toward Hydroponic Wastewaters Remediation. Water, Air, & Soil Pollution 2024;235:422.
[32] Sevim F, Lacin O, Ediz EF, Demir F. Adsorption capacity, isotherm, kinetic, and thermodynamic studies on adsorption behavior of malachite green onto natural red clay. Environmental Progress & Sustainable Energy 2021;40:e13471.
[33] Erdem S, Öztekin M, Açıkel YS. Investigation of tetracycline removal from aqueous solutions using halloysite/chitosan nanocomposites and halloysite nanotubes/alginate hydrogel beads. Environmental Nanotechnology, Monitoring & Management 2021;16:100576.
[34] Douba H, Sabour S, Benatallah L, Fizir M, Mohammedi O. Catalytic Activity of Ti-Modified MCM-41 for Oxidation of Secondary Alcohol with H2O2. Journal of Inorganic and Organometallic Polymers and Materials 2023;33:3259-71.
[35] Zheng S, Fan J, Lu X. Heated kaolinite-La(III) hydroxide complex for effective removal of phosphate from eutrophic water. Applied Clay Science 2023;231:106729.
[36] Chubar N, Gerda V, Szlachta M, Yablokova G. Effect of Fe oxidation state (+ 2 versus+ 3) in precursor on the structure of Fe oxides/carbonates-based composites examined by XPS, FTIR and EXAFS. Solid State Sciences 2021;121:106752.
[37] Tangboriboon N, Kunanuruksapong R, Sirivat A. Preparation and properties of calcium oxide from eggshells via calcination. Materials Science-Poland 2012;30:313-22.
[38] Wu M, Zhao M, Li X, Liang J, Xue Y. Montmorillonite-modified stabilizing SA/CMC gel spheres cross-linked by lanthanum for tetracycline hydrochloride removal. Journal of Water Process Engineering 2023;56:104563.
[39] Zheng S, Fan J, Lu X. Heated kaolinite-La (III) hydroxide complex for effective removal of phosphate from eutrophic water. Applied Clay Science 2023;231:106729.
[40] Jiang G, Cao S, Zheng S, Qin Z, Yan Y, Wu Q, et al. Effect of kaolinite on removal of Pb in simulated wastewater by oxalic acid–activated phosphate rock. Journal of Soils and Sediments 2022;22:1703-12.
[41] Dewi R, Agusnar H, Alfian Z. Characterization of technical kaolin using XRF, SEM, XRD, FTIR and its potentials as industrial raw materials. Journal of Physics: Conference Series: IOP Publishing; 2018. p. 042010.
[42] Aimdate K, Srifa A, Koo-Amornpattana W, Sakdaronnarong C, Klysubun W, Kiatphuengporn S, et al. Natural kaolin-based Ni catalysts for CO2 methanation: On the effect of ce enhancement and microwave-assisted hydrothermal synthesis. ACS omega 2021;6:13779-94.

[43] Rocher V, Siaugue J-M, Cabuil V, Bee A. Removal of organic dyes by magnetic alginate beads. Water research 2008;42:1290-8.
[44] Rassis D, Saguy I, Nussinovitch A. Collapse, shrinkage and structural changes in dried alginate gels containing fillers. Food hydrocolloids 2002;16:139-51.
[45] Roquero DM, Othman A, Melman A, Katz E. Iron (III)-cross-linked alginate hydrogels: A critical review. Materials Advances 2022;3:1849-73.
[46] Marzban N, Moheb A, Filonenko S, Hosseini SH, Nouri MJ, Libra JA, et al. Intelligent modeling and experimental study on methylene blue adsorption by sodium alginate-kaolin beads. International Journal of Biological Macromolecules 2021;186:79-91.
[47] Reddy OS, Subha M, Jithendra T, Madhavi C, Rao KC, Mallikarjuna B. Sodium alginate/gelatin microbeads-intercalated with kaolin nanoclay for emerging drug delivery in wilson's disease. International Journal of Applied Pharmaceutics 2019:71-80.
[48] Zhao Y, Gu X, Gao S, Geng J, Wang X. Adsorption of tetracycline (TC) onto montmorillonite: cations and humic acid effects. Geoderma 2012;183:12-8.
[49] Duan S, Gao Y, Lan G, Qiu H, Xu B, Xie Z, et al. In-situ synthesis of MIL-100 (Fe)@ chitosan composite beads with hierarchical porous structure for efficient adsorption of chlortetracycline hydrochloride: Synthesis, performance and mechanisms. Separation and Purification Technology 2024;333:125938.
[50] Zhao Q, Zhang H, Zhao X, Wang X, Zhang K, Binguo Z, et al. Sodium alginate-based biochar gel spheres: synthesis, structural analysis, and ofloxacin adsorption efficiency. Materials Research Express 2024;11:125507.
[51] Merakchi A. Utilisation des biopolymères modifiés d'origines végétale et animale dans le traitement des eaux: Universite Mouloud MAMMERI Tizi-Ouzou; 2019.
[52] Argun ME, Dursun S, Ozdemir C, Karatas M. Heavy metal adsorption by modified oak sawdust: Thermodynamics and kinetics. Journal of hazardous materials 2007;141:77-85.
[53] Asmaly HA, Abussaud B, Saleh TA, Gupta VK, Atieh MA. Ferric oxide nanoparticles decorated carbon nanotubes and carbon nanofibers: From synthesis to enhanced removal of phenol. Journal of Saudi Chemical Society 2015;19:511-20.
[54] Aliyu M, Abdullah AH, bin Mohamed Tahir MI. Adsorption tetracycline from aqueous solution using a novel polymeric adsorbent derived from the rubber waste. Journal of the Taiwan Institute of Chemical Engineers 2022;136:104333.
[55] He Y, Shi J, Yang Q, Tong Y, Ma Z, Junior LB, et al. Co-doped 3D petal-like ZnIn2S4/GaN heterostructures for efficient removal of chlortetracycline residue from real pharmaceutical wastewater. Chemical Engineering Journal 2022;446:137355.

926 [56] Chang J, Shen Z, Hu X, Schulman E, Cui C, Guo Q, et al. Adsorption of tetracycline by
927 shrimp shell waste from aqueous solutions: adsorption isotherm, kinetics modeling, and
928 mechanism. ACS omega 2020;5:3467-77.
929 [57] da Silva Bruckmann F, Ledur CM, da Silva IZ, Dotto GL, Rhoden CRB. A DFT
930 theoretical and experimental study about tetracycline adsorption onto magnetic graphene
931 oxide. Journal of Molecular Liquids 2022;353:118837.
932 [58] Nasiri A, Rajabi S, Amiri A, Fattahizade M, Hasani O, Lalehzari A, et al. Adsorption of
933 tetracycline using CuCoFe2O4@ Chitosan as a new and green magnetic nanohybrid
934 adsorbent from aqueous solutions: Isotherm, kinetic and thermodynamic study. Arabian
935 Journal of Chemistry 2022;15:104014.
936 [59] Weber Jr WJ, Morris JC. Kinetics of adsorption on carbon from solution. Journal of the
937 sanitary engineering division 1963;89:31-59.
938 [60] Acosta R, Fierro V, De Yuso AM, Nabarlatz D, Celzard A. Tetracycline adsorption onto
939 activated carbons produced by KOH activation of tyre pyrolysis char. Chemosphere
940 2016;149:168-76.
941 [61] Yang X, An M, Han N, Zhang S, Rong Q, Lu H. Study on the adsorption of
942 chlortetracycline in water on peanut shells decorated with magnetic particles by ultrasonic-
943 assisted method. Biomass Conversion and Biorefinery 2025;15:2603-17.
944 [62] Tunç MS, Hanay Ö, Yıldız B. Adsorption of chlortetracycline from aqueous solution by
945 chitin. Chemical Engineering Communications 2020;207:1138-47.
946 [63] Yu R, Yu X, Xue B, Liao J, Zhu W, Tian S. Adsorption of chlortetracycline from
947 aquaculture wastewater using modified zeolites. Journal of Environmental Science and
948 Health, Part A 2020;55:573-84.
949 [64] Zhang D, He Q, Hu X, Zhang K, Chen C, Xue Y. Enhanced adsorption for the removal
950 of tetracycline hydrochloride (TC) using ball-milled biochar derived from crayfish shell.
951 Colloids and Surfaces A: Physicochemical and Engineering Aspects 2021;615:126254.
952 [65] Xiang W, Zhang X, Luo J, Li Y, Guo T, Gao B. Performance of lignin impregnated
953 biochar on tetracycline hydrochloride adsorption: Governing factors and mechanisms.
954 Environmental Research 2022;215:114339.
955 [66] Nguyen CH, Fu C-C, Kao D-Y, Van Tran TT, Juang R-S. Adsorption removal of
956 tetracycline from water using poly (vinylidene fluoride)/polyaniline-montmorillonite mixed
957 matrix membranes. Journal of the Taiwan Institute of Chemical Engineers 2020;112:259-70.

[67] Manzar MS, Ahmad T, Ullah N, Chellam PV, John J, Zubair M, et al. Comparative adsorption of Eriochrome Black T and Tetracycline by NaOH-modified steel dust: Kinetic and process modeling. Separation and Purification Technology 2022;287:120559.
[68] Douba H, Mohammedi O, Cheknane B. Adsorption of rhodamine 6G dye onto Al-MCM-41 and MCM-41 mesoporous materials. Kemija u industriji: Časopis kemičara i kemijskih inženjera Hrvatske 2022;71:569-82.
[69] Rossner A, Snyder SA, Knappe DR. Removal of emerging contaminants of concern by alternative adsorbents. Water research 2009;43:3787-96.
[70] Ebisike K, Okoronkwo AE, Alaneme KK, Akinribide OJ. Thermodynamic study of the adsorption of Cd2+ and Ni2+ onto chitosan–Silica hybrid aerogel from aqueous solution. Results in Chemistry 2023;5:100730.
[71] Ji L, Chen W, Zheng S, Xu Z, Zhu D. Adsorption of sulfonamide antibiotics to multiwalled carbon nanotubes. Langmuir 2009;25:11608-13.
[72] Cheng W, Kalahroodi EL, Marsac R, Hanna K. Adsorption of quinolone antibiotics to goethite under seawater conditions: application of a surface complexation model. Environmental science & technology 2018;53:1130-8.
[73] Hashemzadeh F, Ariannezhad M, Derakhshandeh SH. Sustainable removal of tetracycline and paracetamol from water using magnetic activated carbon derived from pine fruit waste. Scientific Reports 2024;14:16346.
[74] Orhon D, Çokgör EU. COD fractionation in wastewater characterization—the state of the art. Journal of Chemical Technology & Biotechnology: International Research in Process, Environmental AND Clean Technology 1997;68:283-93.
[75] Devi R, Dahiya R. COD and BOD removal from domestic wastewater generated in decentralised sectors. Bioresource Technology 2008;99:344-9.
[76] Akinyemi SA, Nyakuma BB, Adebayo OF, Kayode AT, Hower JCJJoAES. Geochemistry, mineralogy and thermal analyses of Cretaceous coals from the Benue Trough basin Nigeria: Reconnaissance assessments. 2021;178:104167.
[77] Xiaonuo, Zhang, Xiaoyan, Lin, Yan, Chen, et al. Study on adsorption of tetracycline by Cu-immobilized alginate adsorbent from water environment. 2018.
[78] Hu Y, Pan C, Zheng X, Liu S, Peng XJW. Removal of Ciprofloxacin with Aluminum-Pillared Kaolin Sodium Alginate Beads (CA-Al-KABs): Kinetics, Isotherms, and BBD Model. 2020;12:905.
[79] Priya SS, Radha K. A review on the adsorption studies of tetracycline onto various types of adsorbents. Chemical Engineering Communications 2017;204:821-39.

992 [80] Gao Y, Li Y, Zou D. Unraveling the synergistic effect of adsorption-photocatalysis in
993 magnetically recyclable Fe3O4/metal-organic gels/sodium alginate beads for chlortetracycline
994 hydrochloride elimination. Chemical Engineering Journal 2024;480:148049.
995 [81] Chen H, Guo P, Huang Z, Sun J, Lei Y, Xu J. Enhanced stability and conductivity of
996 montmorillonite and sucrose loaded Fe-MOFs for degradation of chlortetracycline
997 hydrochloride via electrochemically activated persulfate. Applied Clay Science
998 2024;249:107231.

999

Supplementary Files

This is a list of supplementary files associated with this preprint. Click to download.

- SI.docx